Design and synthesis of pyrazoleeoxindole conjugates targeting tubulin polymerization as new anticancer agents

ARTICLE *in* EUROPEAN JOURNAL OF MEDICINAL CHEMISTRY · JANUARY 2015

Impact Factor: 3.45

1 AUTHOR:

Anver Basha Shaik

Indian Institute of Chemical Technology

24 PUBLICATIONS **75** CITATIONS

SEE PROFILE

European Journal of Medicinal Chemistry 92 (2015) 501–513

Contents lists available at ScienceDirect

European Journal of Medicinal Chemistry

journal homepage: http://www.elsevier.com/locate/ejmech

Original article

Design and synthesis of pyrazole–oxindole conjugates targeting tubulin polymerization as new anticancer agents

Ahmed Kamal [a,*], Anver Basha Shaik [a], Nishant Jain [b], Chandan Kishor [b], Ananthamurthy Nagabhushana [c,d], Bhukya Supriya [b], G. Bharath Kumar [a], Sumit S. Chourasiya [a], Yerramsetty Suresh [b], Rakesh K. Mishra [c], Anthony Addlagatta [b,*]

[a] Medicinal Chemistry and Pharmacology, CSIR – Indian Institute of Chemical Technology, Hyderabad 500007, India
[b] Centre for Chemical Biology, CSIR – Indian Institute of Chemical Technology, Hyderabad 500007, India
[c] CSIR – Centre for Cellular and Molecular Biology, Hyderabad 500007, India
[d] CoE in Epigenetics, IISER-Pune, Pune 411021, India

ARTICLE INFO

Article history:
Received 4 June 2013
Received in revised form
29 October 2013
Accepted 31 October 2013
Available online 8 November 2013

Keywords:
Pyrazole–oxindole conjugates
Tubulin depolymerization
Zebrafish screening and molecular modeling

ABSTRACT

A series of twenty one compounds with pyrazole and oxindole conjugates were synthesized by Knoevenagel condensation and investigated for their antiproliferative activity on different human cancer cell lines. The conjugates are comprised of a four ring scaffold; the structural isomers **12b** and **12c** possess chloro-substitution in the D ring. Among the congeners **12b**, **12c**, and **12d** manifested significant cytotoxicity and inhibited tubulin assembly. Treatments with **12b**, **12c** and **12d** resulted in accumulation of cells in G2/M phase, disruption of microtubule network, and increase in cyclin B1 protein. Zebrafish screening revealed that **12b**, and **12d** caused developmental defects. Docking analysis demonstrated that the congeners occupy the colchicine binding pocket of tubulin.

1. Introduction

Microtubules, composed of αβ-tubulin heterodimers, are major constituents of the cytoskeleton in eukaryotic cells. The α- and β-tubulins are among the most highly conserved eukaryotic proteins [1]. Microtubules are pleiotropic in their function, particularly in organizing the spatial distribution of organelles in cells and chromosomes during cell division. Due to their essential functions in the cell, microtubules serve as an attractive drug target [2]. The dynamic equilibrium between microtubule polymerization and depolymerization is central to most of microtubule mediated functions including cell division [3]. This attribute has been exploited by numerous natural products and synthetic molecules which function as tubulin binding agents (TBAs) [4]. The microtubules posses three sites for ligand binding the vinca domain, colchicine domain and taxol domain. However, occurrence of peripheral neuropathy is a major limitation in development of antimicrotubule agents as drugs [5]. Therefore, discovery of novel molecules is required to overcome multi-drug resistance and neuropathies.

Oxindoles are important pharmacophores that are known to enhance anticancer activity of some established molecules. Sunitinib (**5**) and indirubin (**6**) are established anticancer agents containing oxindole as the basic scaffold (Fig. 1A) [6–8]. Recently, it has been observed that chromone–pyrimidine, chromone–indolinone, chromone–pyrazole, indole–pyrimidine, indole–indolinone and indole–pyrazole conjugates demonstrated profound growth inhibitory activity against different cancer cells [9]. Moreover substituted indolin-2-ones are potential inhibitors of p90 ribosomal S6 protein kinase [10]. In addition, tri and tetra substituted pyrazole derivates proved to have potent anticancer action due to the inhibition of p38α MAP kinase [11]. Whereas 4-arylazo-3,5-diamino-1*H*-pyrazoles function as novel group of ATP antagonists with moderate potency against CDK2–cyclin E complex [12]. The anticancer effects of some pyrazole amide derivatives are mediated by inhibition of the Elk-3 pathway and effects microtubules [13].

The unique feature of microtubule-binding agents, in contrast to other categories of anticancer drugs, is their incredible structural complexity and diversity, which provides many possibilities for

* Corresponding authors. Tel.: +91 40 27193157; fax: +91 40 27193189.
E-mail addresses: ahmedkamal@iict.res.in (A. Kamal), anthony@iict.res.in (A. Addlagatta).

0223-5234/$ – see front matter © 2013 Elsevier Masson SAS. All rights reserved.
http://dx.doi.org/10.1016/j.ejmech.2013.10.077

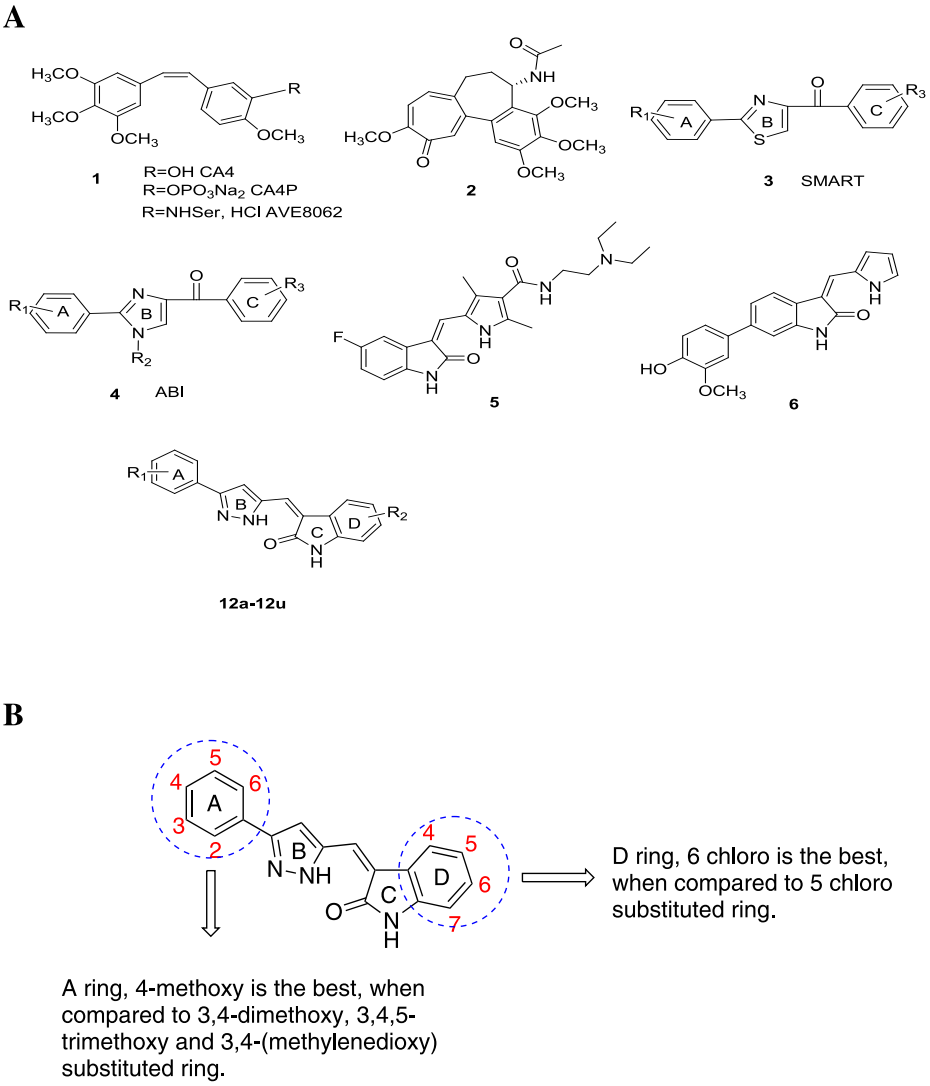

Fig. 1. A. Structures of some anticancer molecules Combretastatin (**1**), colchicine (**2**), substituted methoxylbenzoyl-aryl-thiazole (SMART) (**3**), 2-aryl-4-benzoyl-imidazole series (ABI) (**4**), Sunitinib (**5**), indirubin (**6**) and pyrazole–oxindole conjugates (**12a**–**u**). B. SAR of pyrazole–oxindole conjugates (see Table 1 for R_1, R_2).

optimization and new scaffold design. Combretastatin (**1**) and colchicine (**2**) possess a two ring and three ring scaffolds with a trimethoxyphenyl group for anchorage, which efficiently inhibit tubulin polymerization. Based on the ring geometry, the substituted methoxylbenzoyl-aryl-thiazole (SMART) (**3**) series contain a basic three ring scaffold and functions as tubulin inhibitors [14]. Due to limited water solubility, the core thiazole ring was modified to imidazole to generate 2-aryl-4-benzoyl-imidazole series (ABI) (**4**) (Fig. 1A) [15]. Nevertheless, the three ring (A, B and C) based scaffolds can be exploited further to generate better antitubulin molecules that could affect tubulin polymerization. Earlier we reported that oxindole derived imidazopyrazines exhibit significant anticancer activity [16]. In the present study, we performed the synthesis of (*Z*)-3-((3-phenyl-1*H*-pyrazol-5-yl) methylene) indolin-2-ones employing Knoevenagel condensation to generate a four ring scaffold (A: methoxy/methylene dioxy, B: pyrazole, C, D: oxindole). The congeners (**12a**–**u**) were functionalized at A ring and D ring with various substituents such as methoxy, methylene dioxy, chloro, fluoro and nitro groups (Fig. 1A).

2. Results and discussion

2.1. Chemistry

The Synthesis of (*Z*)-3-((3-phenyl-1*H*-pyrazol5yl)methylene) indolin-2-one analogs **12**(**a**–**u**) described in the study are outlined in Scheme 1. The final step has been carried out by means of Knoevenagel condensation between an equimolar mixture of oxindole/indolinone and 3-substituted phenyl-1*H*-pyrazole-5-carbaldehydes **11**(**a**–**d**) in the presence of piperdine in ethanol [6,9,10]. The key intermediates 3-substituted phenyl-1H-pyrazole-5-carbaldehydes **11**(**a**–**d**) was prepared in four sequential steps. Initially substituted acetophenones **7**(**a**–**d**) reacted with diethyl oxalate in the presence of sodium ethanolate in ethanol yielded ethyl 2,4-dioxo-4-(substituted phenyl)butanoates **8**(**a**–**d**). This was further cyclized with NH_2–$NH_2 \cdot 2HCl$ in ethanol to produce ethyl 3-substituted phenyl-1*H*-pyrazole-5-carboxylates **9**(**a**–**d**) in good yields [17,18]. The obtained carboxylates were reduced to (3-substitutedphenyl-1H-pyrazol-5-yl) methanols **10**(**a**–**d**) by $LiAlH_4$.

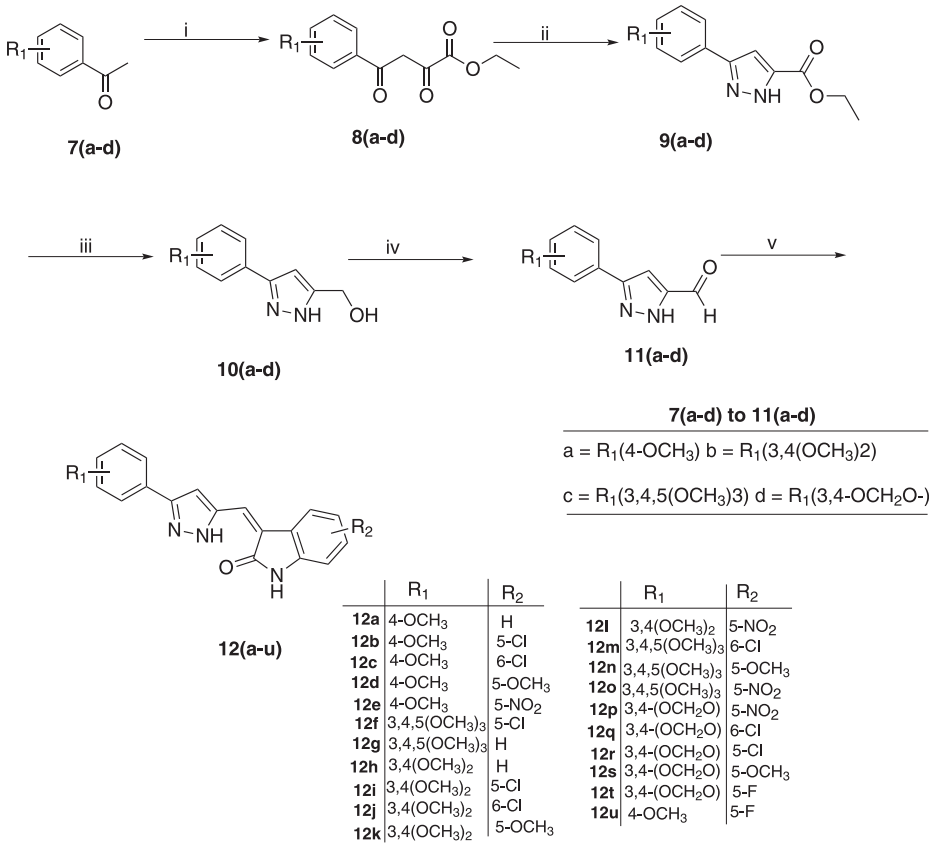

	R_1	R_2
12a	4-OCH_3	H
12b	4-OCH_3	5-Cl
12c	4-OCH_3	6-Cl
12d	4-OCH_3	5-OCH_3
12e	4-OCH_3	5-NO_2
12f	3,4,5-$(OCH_3)_3$	5-Cl
12g	3,4,5-$(OCH_3)_3$	H
12h	3,4-$(OCH_3)_2$	H
12i	3,4-$(OCH_3)_2$	5-Cl
12j	3,4-$(OCH_3)_2$	6-Cl
12k	3,4-$(OCH_3)_2$	5-OCH_3
12l	3,4-$(OCH_3)_2$	5-NO_2
12m	3,4,5-$(OCH_3)_3$	6-Cl
12n	3,4,5-$(OCH_3)_3$	5-OCH_3
12o	3,4,5-$(OCH_3)_3$	5-NO_2
12p	3,4-(OCH_2O)	5-NO_2
12q	3,4-(OCH_2O)	6-Cl
12r	3,4-(OCH_2O)	5-Cl
12s	3,4-(OCH_2O)	5-OCH_3
12t	3,4-(OCH_2O)	5-F
12u	4-OCH_3	5-F

Scheme 1. Synthesis of pyrazole–oxindole conjugates (**12a**–**u**): *Reagents and conditions*: (i) NaOEt/EtOH, 4 h, 0 °C–rt, 68%; (ii) NH_2–NH_2·2HCl/EtOH, 3 h, reflux, 72–79%; (iii) $LiAlH_4$/THF, 1 h 0 °C–rt, 51–70%. (iv) IBX/DMSO, 1 h, rt, 51–70% (v) oxindoles/EtOH, 4 h, reflux, 51–70%.

These were selectively oxidized to 3-substituted phenyl-1*H*-pyrazole-5-carbaldehydes **11**(**a**–**d**) by IBX in DMSO.

2.2. Evaluation of biological activity

2.2.1. Antiproliferative activity

The cell lines used were, HeLa (cervical carcinoma), A549 (non-small cell lung cancer), MCF-7 (breast cancer) and DU145 (prostate carcinoma) cell lines; the results are shown in Table 1. To determine the structure–activity relationships on the phenyl A ring and the oxindole D ring, we introduced various groups on both the rings. Among the compounds investigated **12b**, **12c**, and **12d** showed promising anticancer activity against all the cell lines tested. Nocodazole was employed as standard drug. Interestingly the active compounds **12b** and **12c** are structural isomers with chloro substitutions at 5 and 6 of D ring with a mono methoxy at A ring. These structural isomers **12b** and **12c** exhibited IC_{50} values of 6 μM and 3 μM respectively; with a maximal activity in HeLa cells (The IC_{50} value for each compound is the average of all four cancer cell lines). In contrast, **12d** (IC_{50}: 7.5 μM) with a mono methoxy substitution A and D ring also exhibited strong activity in HeLa cells. The presence of bulkier groups in the A and D ring of **12k** (IC_{50}: 23.5 μM), **12n** (IC_{50}: 16.7 μM) and **12s** (IC_{50}: 20.3 μM) decreased the activity of the molecules. The replacement of chloro with flouro in the compounds **12t** and **12u** in the D ring showed deleterious effect on the activity with IC_{50} of 28.7 μM and 33 μM respectively. The compounds devoid of any substitutions (**12a**, **12g** and **12h**) in the ring D demonstrated better antiproliferative activity, when compared to **12e**, **12l**, **12o** and **12p** carrying an electron withdrawing group. Based on structural variation, the optimal order of substitutions on the A ring is mono methoxy > dimethoxy > 3,4-(methylenedioxy) > trimethoxy. The compounds **12b** (IC_{50}: 8.1 μM), **12c** (IC_{50}: 5.9 μM) and **12d** (IC_{50}: 9.2 μM) displayed remarkable inhibition of tubulin polymerization, which positively correlated with antiproliferative activity (Table 2). As expected, Nocodazole significantly inhibited tubulin polymerization in our assays. Intriguingly, the compound **12b** and **12c** displayed differences in their binding interactions with tubulin due to the shift in chloro substitution. In comparison, the other analogs showed partial effect on tubulin polymerization. Therefore, results suggest that the presence of a mono methoxy group in A ring and chloro or methoxy group in D ring resulted in promising molecules, which exhibit potent anticancer activity and down regulate tubulin polymerization (Fig. 1B) and their order of activities are **12c** > **12b** > **12d**.

2.2.2. Effect on cell cycle arrest

To elucidate whether the cytoxicity induced by the derivatives was due to cell cycle arrest, we performed flow cytometry analysis for derivatives that exhibited potent cytotoxicity and significantly inhibited tubulin assembly. HeLa cells were treated with **12b**, **12c** and **12d** at 5 μM and 10 μM for 24 h. The cells accumulated in G2/M phase in a concentration dependent manner. Cells treated with **12c** at 10 μM showed 79% arrest of cells in G2/M phase. In comparison, HeLa cells treated with **12b** or **12d** at 10 μM resulted in an increase of mitotic cells by 60% and 72% respectively (Fig. 2).

Table 1
Structures of the compounds **12a**–**u** and *in vitro* antiproliferative activity.

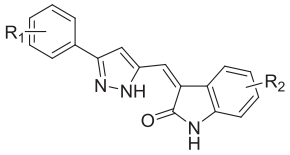

	R_1	R_2	$IC_{50} \pm SEM$ (μM)				
			HeLa	A549	MCF7	DU145	Average
12a	4-OCH_3	H	18.0 ± 0.6	14.0 ± 0.4	15.0 ± 0.3	21.0 ± 0.5	17
12b	4-OCH_3	5-Cl	5.0 ± 0.7	6.0 ± 1.3	9.3 ± 0.3	4.0 ± 2.1	6.0
12c	4-OCH_3	6-Cl	2.4 ± 0.8	3.0 ± 0.6	3.6 ± 0.4	3.0 ± 1.9	3.0
12d	4-OCH_3	5-OCH_3	7.1 ± 0.3	8.0 ± 0.2	6.0 ± 0.3	9.0 ± 3.2	7.5
12e	4-OCH_3	5-NO_2	33.0 ± 0.4	22.0 ± 0.3	24.0 ± 2.1	26.0 ± 4.6	26.2
12f	3,4,5(OCH_3)$_3$	5-Cl	12.0 ± 0.1	27.0 ± 0.1	44.0 ± 0.7	21.0 ± 2.1	26.0
12g	3,4,5(OCH_3)$_3$	H	21.0 ± 0.2	21.0 ± 0.2	27.0 ± 2.1	35.0 ± 5.1	26.0
12h	3,4,(OCH_3)$_2$	H	21.0 ± 0.2	29.0 ± 0.3	36.0 ± 2.8	31.0 ± 6.7	29.2
12i	3,4,(OCH_3)$_2$	5-Cl	10.0 ± 0.8	24.0 ± 0.1	16.0 ± 0.1	21.0 ± 1.2	17.7
12j	3,4,(OCH_3)$_2$	6-Cl	11.0 ± 0.2	18.0 ± 5.6	27.0 ± 0.2	13.9 ± 1.6	17.4
12k	3,4,(OCH_3)$_2$	5-OCH_3	13.0 ± 0.3	15.0 ± 1.6	32.0 ± 0.7	34.0 ± 2.3	23.5
12l	3,4,(OCH_3)$_2$	5-NO_2	36.0 ± 0.6	42.0 ± 2.4	42.0 ± 2.2	28.0 ± 5.9	37.0
12m	3,4,5(OCH_3)$_3$	6-Cl	11.0 ± 0.4	33.0 ± 0.6	22.0 ± 0.4	27.0 ± 2.7	23.2
12n	3,4,5(OCH_3)$_3$	5-OCH_3	16.0 ± 0.3	33.0 ± 1.3	8.8 ± 0.6	9.1 ± 0.3	16.7
12o	3,4,5(OCH_3)$_3$	5-NO_2	30.0 ± 0.5	22.0 ± 0.3	16.0 ± 0.4	20.0 ± 0.6	22.0
12p	3,4-(OCH_2O)	5-NO_2	24.0 ± 0.3	37.0 ± 0.4	17.0 ± 0.6	36.0 ± 0.6	28.5
12q	3,4-(OCH_2O)	6-Cl	7.3 ± 1.8	27.0 ± 0.5	18.0 ± 0.2	24.0 ± 4.5	19.0
12r	3,4-(OCH_2O)	5-Cl	12.0 ± 0.1	29.0 ± 1.8	44.0 ± 0.7	24.0 ± 2.1	27.2
12s	3,4-(OCH_2O)	5-OCH_3	13.5 ± 1.2	24.0 ± 3.2	9.8 ± 0.3	34.0 ± 1.1	20.3
12t	3,4-(OCH_2O)	5-F	32.0 ± 0.4	26.0 ± 3.1	36.0 ± 1.5	21.0 ± 5.2	28.7
12u	4-OCH_3	5-F	22.0 ± 0.2	29.0 ± 1.8	36.0 ± 3.1	25.0 ± 6.7	28.0
Nocodazole			1.1 ± 0.5	0.89 ± 0.01	1.7 ± 0.65	3.2 ± 0.83	1.72

Cell lines were treated with different concentrations of compounds for 48 h as described under Experimental protocol. Cell viability was measured employing MTT assay. IC50 values are indicated as the mean of three independent experiments.

2.2.3. *Effect of **12b**, **12c** and **12d** on microtubule network*

Presence of aberrant spindle fibers due to altered microtubule dynamics is a hallmark of cells treated with anti-mitotic agents [19]. In order to ascertain if the cell cycle arrest is due to spindle abnormality, HeLa cells treated with 5 μM concentrations of **12b**, **12c** and **12d** were stained with tubulin antibody. The control treated cells exhibit an organized network of microtubules. In contrast cells exposed with **12b**, **12c** showed multipolar spindle fibers, and **12d** treated cells exhibit a metaphase arrest (Fig. 3).

2.2.4. *Effect of **12b**, **12c** and **12d** on cellular tubulin polymerization*

These observations suggest that the aberrant spindle dynamics in cells treated with **12b**, **12c** and **12d** results in cell cycle arrest. Tubulin assembly assays reveal that the congeners inhibit microtubule polymerization, consequently we analyzed for their effect on cellular tubulin. To elucidate this, HeLa cells were treated with **12b**, **12c** and **12d** at 5 μM concentrations for 24 h. Subsequently, cells were permeabilized to collect the soluble fraction and remaining cells were collected as the polymerized fraction. Immunoblot analysis revealed that the cells exposed to pyrazole–oxindole conjugates contained more tubulin in the soluble fraction of cells. Therefore, increased tubulin in soluble fraction of cells treated with pyrazole–oxindole conjugates corroborated with the inhibition of tubulin assembly and arrest of cells in G2/M phase (Fig. 4A). To further validate our observations that pyrazole–oxindole conjugates function as microtubule inhibitors, cells treated with the selected analogs demonstrated increased amount of cyclin B1 protein, a G2/M marker (Fig. 4B).

Table 2
Antitubulin activity of compounds **12a**–**u**.

Compound	Inhibition of tubulin polymerization (μM)	Compound	Inhibition of tubulin polymerization (μM)
12a	38.9 ± 1.90	**12l**	18.0 ± 0.71
12b	8.10 ± 0.61	**12m**	22.4 ± 1.23
12c	5.90 ± 0.78	**12n**	16.0 ± 1.10
12d	9.2 ± 1.10	**12o**	15.3 ± 4.10
12e	21.0 ± 1.10	**12p**	14.7 ± 2.10
12f	25.3 ± 2.30	**12q**	14.5 ± 2.30
12g	18.0 ± 0.63	**12r**	35.3 ± 2.30
12h	23.0 ± 1.90	**12s**	12.0 ± 0.89
12i	33.8 ± 1.60	**12t**	24.0 ± 0.56
12j	18.9 ± 0.89	**12u**	25.0 ± 0.59
12k	22.1 ± 2.50	**Nocodazole**	2.2 ± 0.66

Effect of congeners on tubulin polymerization. IC_{50} values for **12a** to **12u** were determined from the tubulin polymerization assays.

2.3. *Effect of **12a**, **12b**, **12c** and **12d** on zebrafish development*

Zebrafish (Danio rerio) has emerged as a powerful model system for chemical genetics [20–22]. In order to validate antiproliferative effect of these compounds *in vivo*, their effects on development of zebrafish embryos was examined. Most of the compounds screened had little or no effect on development at 25 μM. However, embryos treated with **12b** exhibited marked delay in development. Its isomer **12c** has a mild effect on the development of zebrafish embryos, highlighting possible differential ADME (absorption, distribution, metabolism, excretion) properties of the ring substitutes *in vivo*. Embryos treated with **12a** also showed delay in the development. This could be due to better absorption and/or bioavailability of the compound *in vivo* or due to additional and/or different target/s and needs further investigation [23]. Microtubule inhibitors like nocadozole also exhibit such developmental delays (Fig. 5). These

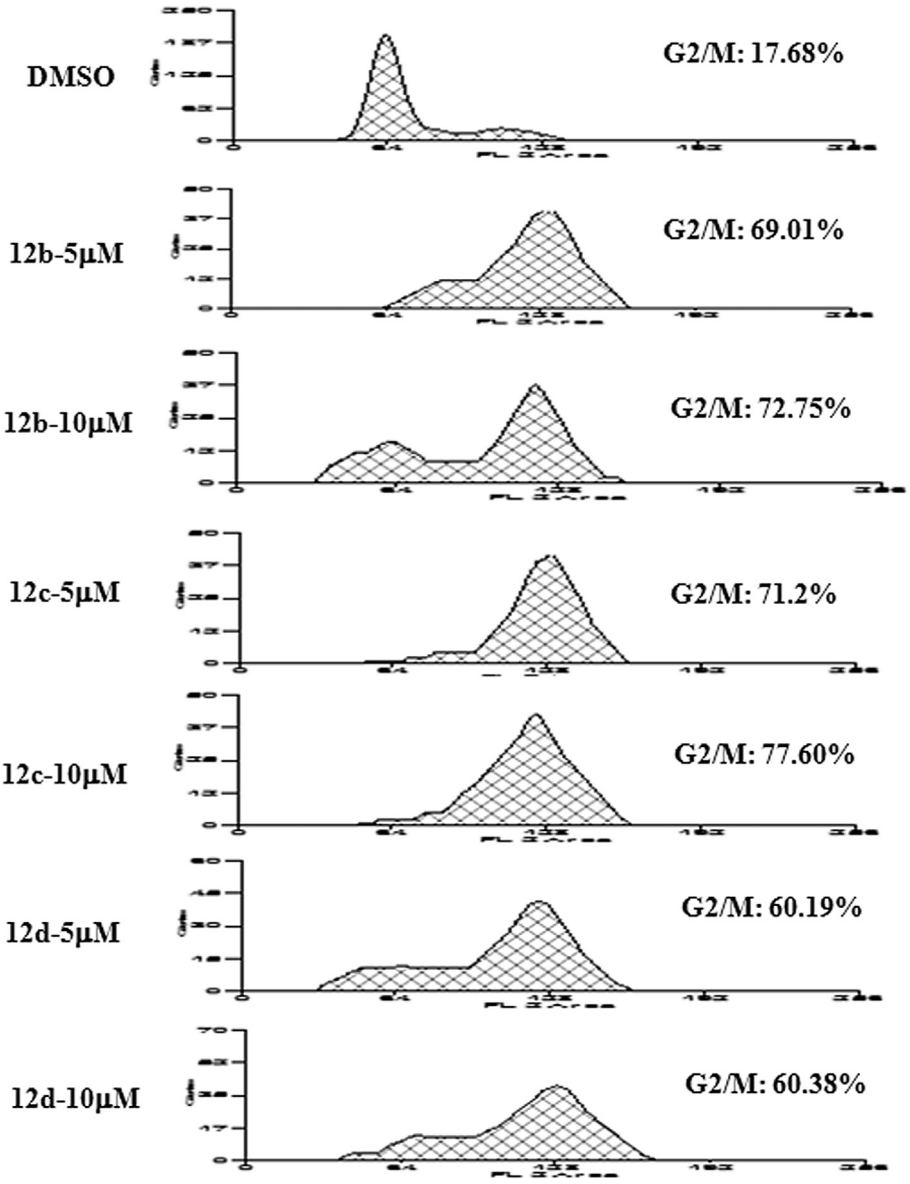

Fig. 2. Anti-mitotic effects of **12b**, **12c**, and **12d** by FACS analysis: Induction of cell cycle G2/M arrest by compound **12b**, **12c**, and **12d**. HeLa cells were harvested after treatment at 5 μM and 10 μM for 24 h. Untreated cells and DMSO treated cells served as controls. The percentage of cells in each phase of cell cycle was quantified by flow cytometry.

results suggest that **12b** acts as an anti-mitotic compound in zebrafish embryos and could thus be a potential therapeutic scaffold along with **12c** and **12d**.

2.4. Molecular modeling

In order to examine the interaction of these conjugates in colchicine binding domain of tubulin, Autodock has been employed and three lead compounds (**12b**, **12c** and **12d**) have been docked against the tubulin structure (PDB code: 3E22) [24–27]. The colchicine site is generally buried in the intermediate domain of the β-subunit, surrounded by two β-strands, two helices and a loop, which we label as A-site. Colchicine also interacts with parts of the neighboring α-subunit, which is labeled as B-site, which is wider than the A-site. The A-ring in the current study binds in the A-site of the tubulin while the C and D-rings are placed near the B-site in a slightly different environment compared to the colchicine. A strong hydrogen bond is noted between the carbonyl of the C-ring in the oxindole moiety. Lys254 from β-subunit and Asn101 of α-subunit are involved in placing the oxindole moiety between the two subunits. Although the trimethoxy benzene group is identified as signature for binding to tubulin, we noted that mono methoxy derivatives of our molecules inhibit the tubulin polymerization better than the di and trimethoxy derivatives. This could be due to the strong hydrogen bond with the oxindole moiety in B-site that may affect the binding of the methoxy-substituted benzene in the A-site. Also, within the mono methoxy substituted molecule, inhibition efficiency of tubulin polymerization varied. The C and D rings are buried at the interface of the two subunits of tubulin (Fig. 6). Specifically, the D ring is sandwiched between the Leu248 and Lys352 of β-subunit and Ser178 of α-subunit. This region is narrow and hydrophobic which limits the binding of larger or charged group on the D ring. A chlorine atom at position six in D ring inhibits the tubulin polymerization better than when it is

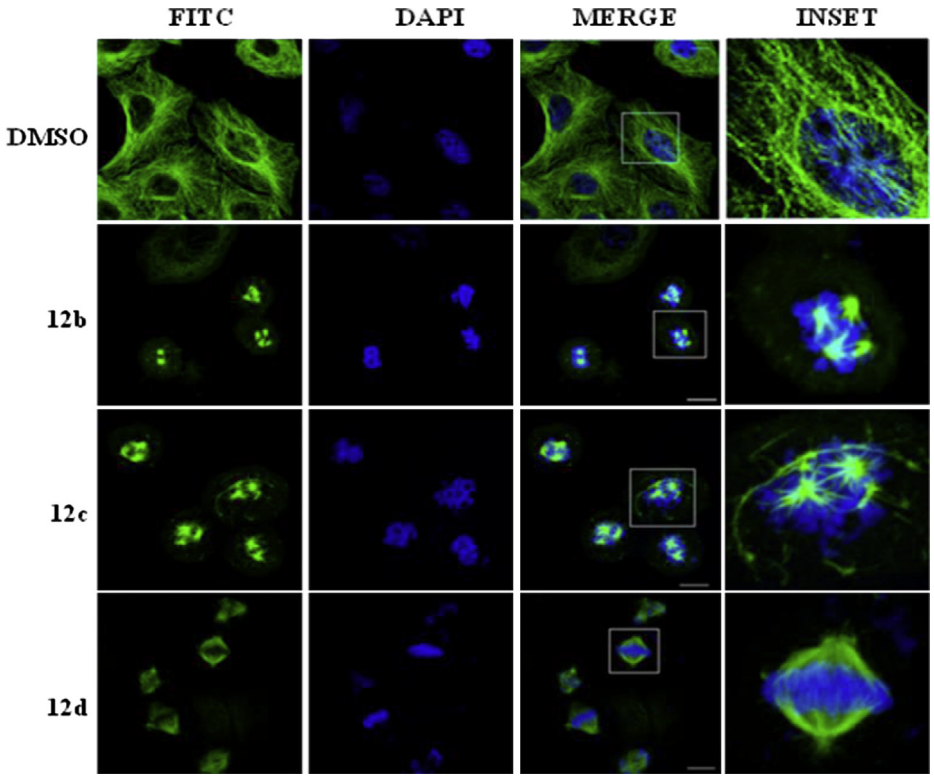

Fig. 3. Effect of **12b**, **12c**, and **12d** on microtubules and nuclear condensation: HeLa cells were independently treated with **12b**, **12c** and **12d** at 5 μM concentrations for 24 h. Following the termination of experiment, cells were fixed and stained for tubulin. DAPI was used as counter stain. The merged images of cells stained for tubulin and DAPI are represented.

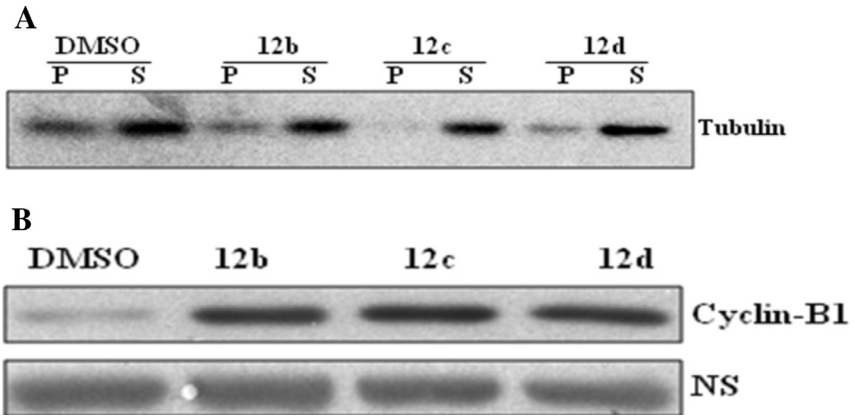

Fig. 4. Distribution of tubulin in polymerized vs soluble fractions as analyzed by immunoblotting in **12b**, **12c**, **12d** treated HeLa cells: A. HeLa cells were treated with 5 μM of **12b**, **12c** and **12d** for 24 h. Tubulin was detected by Immunoblot analysis. B. Hela cells were treated with 5 μM concentrations of compound **12b**, **12c**, and **12d** for 24 h. Subsequently, whole lysates were prepared and analyzed for Cyclin-B1. A non-specific (NS) band at 90 kDa was used as control.

placed at position five. This data also corroborates that all the nitro substituted molecules are comparatively less active (Table 1).

3. Conclusion

In summary, we synthesized new class of pyrazole–oxindole conjugates comprised of a four ring scaffold, which was extensively modified at A and D ring. Majority of the compounds exhibited significant antiproliferative activity where in the presence of a single chloro or methoxy group at D ring was necessary for potent antitubulin activity. The compounds **12b**, **12c** and **12d** stalled cells in G2/M phase and prevented chromosomal separation. Higher levels of Cyclin B1 protein and tubulin in the soluble fraction of cells excellently corroborated with antitubulin activity of the compounds. Zebrafish screening assays demonstrated the congeners affect the normal development of embryos. Molecular modeling analysis revealed that the compounds dock to the colchicine binding site of tubulin. Based on the results, the design and synthesis of the compounds containing pyrazole–oxindole moiety are effective tubulin polymerization inhibitors, which can be further amenable for generation of different conjugates as potential anticancer drugs.

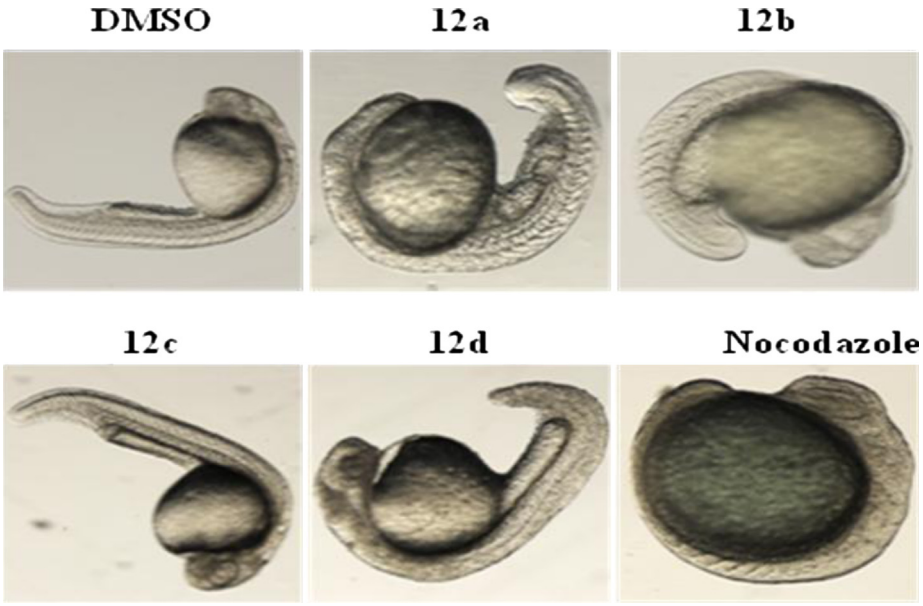

Fig. 5. Effect of microtubule inhibitors on development of zebrafish embryos: Zebrafish embryos were treated with (a) DMSO (1%), **12a**, **12b**, **12c** and **12d** or Nocodazole at 5 hpf. The embryos were imaged at 30 hpf to observe morphological changes.

3.1. Experimental protocols

3.1.1. General

All chemicals and reagents were obtained from Aldrich (Sigma–Aldrich, St. Louis, MO, USA), Lancaster (Alfa Aesar, Johnson Matthey Company, Ward Hill, MA, USA), or Spectrochem Pvt. Ltd. (Mumbai, India) and were used without further purification. Reactions were monitored by TLC performed on silica gel glass plates containing 60 GF-254, and visualization was achieved by UV light or iodine indicator. Column chromatography was performed with Merck 60–120 mesh silica gel. ^{1}H NMR spectra were recorded on Bruker UXNMR/XWIN-NMR (300 MHz) or Inova Varian-VXR-unity (400, 500 MHz) instruments. ^{13}C NMR spectra were recorded on Bruker UXNMR/XWIN-NMR (75 MHz) instrument. Chemical shifts (d) are reported in ppm downfield from an internal TMS standard. ESI spectra were recorded on a Micro mass Quattro LC using ESI+ software with capillary voltage 3.98 kV and ESI mode positive ion trap detector. High-resolution mass spectra (HRMS) were recorded on a QSTAR XL Hybrid MS–MS mass spectrometer. Melting points were determined with an Electro thermal melting point apparatus, and are uncorrected.

3.1.2. Preparation of ethyl 2,4-dioxo-4-(substituted phenyl) butanoates 8(a–d)

Diethyl oxalate (1.0 mol) was added to freshly prepared sodium ethanolate at 0 °C after 10 min substituted acetophenones **7**(**a**–**d**) (1.0 mol) were added slowly in small portions maintaining the temperature 0 °C. After completion of addition the stirring was continued at room temperature for 4 h the reaction mixture was neutralized by diluted H_2SO_4 and extracted with ethyl acetate to offered solid products **8**(**a**–**d**) (yield 85–90%) which were taken as such for the next step without purification.

3.1.3. Preparation of ethyl 3-substituted phenyl-1H-pyrazole-5-carboxylates 9(a–d)

To each ethyl 2, 4-dioxo-4-(substituted phenyl) butanoates **8**(**a**–**d**) (1.0 mol) which were obtained in the earlier step was added hydrazine dihydrochloride (NH_2–NH_2·2HCl) (1.5 mol) in ethanol and heated to reflux for 3 h. The solvent was removed under vacuum then added water to the residue and the compound was extracted with ethyl acetate (50 ml × 4). The organic layer was dried on anhydrous $NaSO_4$ and evaporated the solvent to obtain crude product that was further purified by column chromatography using ethyl acetate and hexane. The pure compounds **9**(**a**–**d**) were eluted at 30–40% of ethyl acetate with good yields.

*3.1.3.1. Ethyl 3-(4-methoxyphenyl)-1H-pyrazole-5-carboxylate (**9a**).* Yellow colored solid; (yield 80.0%): R_f = 0.3 (30% ethyl acetate/hexane); ^{1}H NMR (300 MHz, $CDCl_3$); δ 1.23–1.37 (t, 3H, J_1 = 6.7 Hz, J_2 = 7.5 Hz, –C**H**$_3$), 3.81 (s, 3H, –OC**H**$_3$), 4.17–4.36 (q, 2H, J_1 = 6.7 Hz, J_2 = 7.5 Hz, C**H**$_2$), 6.8 (s, 1H, Ar**H**), 6.90 (d, 2H, J = 2.2 Hz, Ar**H**), 7.62 (d, 2H, J = 9.0 Hz, Ar**H**) ppm; MS (ESI) m/z 247 [M + H].

3.1.3.2. Ethyl 3-(3,4-dimethoxyphenyl)-1H-pyrazole-5-carboxylate 9(b). Pale yellow colored solid; (yield 80.0%): R_f = 0.3 (30% ethyl acetate/hexane); ^{1}H NMR (300 MHz, $CDCl_3$); δ 1.23–1.31 (t, 3H, J_1 = 7.1 Hz, –C**H**$_3$), 3.85 (s, 3H, –OC**H**$_3$), 3.90 (s, 3H, –OC**H**$_3$), 4.19–4.32 (q, 2H, J_1 = 7.1 Hz, –C**H**$_2$), 6.88 (d, 1H, J_1 = 7.1 Hz, –Ar**H**), 6.94 (s, 1H, Ar**H**), 7.21–7.28 (m, 1H, Ar**H**), 7.29–7.34 (m, 1H, Ar**H**), 9.67 (brs, 1H, –N**H**) ppm; MS (ESI) m/z 277 [M + H].

3.1.3.3. Ethyl 3-(3,4,5-trimethoxyphenyl)-1H-pyrazole-5-carboxylate 9(c). Yellow colored solid (yield 75.0%): R_f = 0.3 (40% ethyl acetate/hexane); ^{1}H NMR (300 MHz, $CDCl_3$); δ 1.33–1.40 (t, 3H, J_1 = 6.7 Hz, J_2 = 7.5 Hz, –C**H**$_3$), 3.88 (s, 3H, –OC**H**$_3$), 3.95 (s, 6H, –OC**H**$_3$), 4.33–4.45 (q, 2H, J_1 = 6.7 Hz, J_2 = 7.5 Hz, C**H**$_2$), 7.01 (s, 2H, Ar**H**), 7.05 (s, 1H, Ar**H**) ppm; MS (ESI) m/z 307 [M + H].

3.1.3.4. Ethyl 3-(benzo[d][1,3]dioxol-5-yl)-1H-pyrazole-5-carboxylate 9(d). Pale yellow colored solid (yield 75.0%): R_f = 0.3 (40% ethyl acetate/hexane); ^{1}H NMR (500 MHz, $CDCl_3$); δ 1.33–1.40 (t, 3H, J_1 = 6.7 Hz, J_2 = 7.5 Hz, –C**H**$_3$), 4.33–4.45 (q, 2H, J_1 = 6.7 Hz, J_2 = 7.5 Hz, C**H**$_2$), 6.0 (s, 2H, OC**H**$_2$O), 6.86 (d, 1H, J = 8.3 Hz, Ar**H**), 7.05 (s, 1H, Ar**H**), 7.21–7.28 (m, 2H, Ar**H**) ppm; MS (ESI) m/z 261 [M + H].

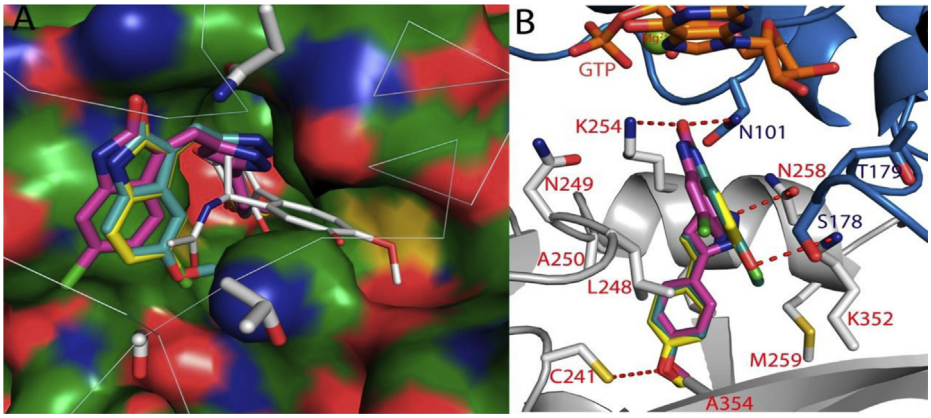

Fig. 6. *Panel A*, Docking pose of **12b** (yellow), **12c** (magentas), **12d** (cyan). The green surface represents β-chain while the gray line diagram indicates the α-chain of tubulin. The 4-methoxybenzene moiety of all the compounds is buried in hydrophobic pocket of colchicine binding domain (A-site). *Panel B*, Stick representation of selected amino acids of α and β subunits of tubulin interacting with compound **12b**, **12c** and **12d**. Gray color for the b-chain and blue for the a-chain of tubulin was used for representation. Red dotted lines indicate the hydrogen bonds. (For interpretation of the references to color in this figure legend, the reader is referred to the web version of this article.)

*3.1.4. Preparation of (3-substitutedphenyl-1H-pyrazol-5-yl) methanols **10**(**a**–**d**)*

To the ethyl 3-substituted phenyl-1*H*-pyrazole-5-carboxylates **9**(**a**–**d**), obtained in the above step was added $LiAH_4$ (0.5 mol) in dry THF at 0 °C and stirred for 1 h at room temperature. Added saturated NH_4Cl solution drop wise to quench the unreacted $LiAlH_4$ and removed the THF under vacuum then extracted with ethyl acetate (100 ml × 4). The organic layer was dried on anhydrous $NaSO_4$ and evaporated ethyl acetate to obtain color less solid products of (3-substitutedphenyl-1*H*-pyrazol-5-yl)methanols **10**(**a**–**d**) (yield 70–80%). The alcohols produced in this step were pure, and no further purification was required. These compounds were taken as such for the next step.

*3.1.5. Preparation of 3-subtitutedphenyl-1H-pyrazole-5-carbaldehydes **11**(**a**–**d**)*

To the (3-substitutedphenyl-1*H*-pyrazol-5-yl)methanols **10**(**a**-**d**) produced in the above step was added IBX (1.2 mol) in DMSO and stirred for 1 h at room temperature. Added ice cold water to the reaction mixture and extracted with ethyl acetate (50 ml × 4). The organic layer was dried on anhydrous $NaSO_4$ and evaporated the ethyl acetate to obtain pure corresponding 3-subtitutedphenyl-1*H*-pyrazole-5-carbaldehydes **11**(**a**–**d**) in good yields (80–85%). The obtained carbaldehydes were as such taken in the next step for the synthesis of pyrazole–oxindole conjugates **12a**–**u**.

*3.1.5.1. 3-(4-Methoxyphenyl)-1H-pyrazole-5-carbaldehyde (**11a**).* 3-(4-methoxyphenyl)-1*H*-pyrazole-5-carbaldehyde **11a** was prepared using above method by the addition of (3-(4-methoxyphenyl)-1*H*-pyrazol-5-yl)methanol **10a** (2.04 g, 10 mmol) IBX (3.36 g, 1.2 mmol). Yellow colored solid (1.71 g, yield 85%): R_f = 0.3 (40% ethyl acetate/hexane); ^{1}H NMR (400 MHz, $CDCl_3$); δ 3.85 (s, 3H, −OC**H**$_3$), 7.78–7.82 (m, 1H, Ar**H**), 7.86–7.93 (m, 2H, Ar**H**), 7.95–8.03 (m, 2H, Ar**H**), 9.95 (s, 1H, C**H**O) ppm; MS (ESI) *m*/*z* 203 [M + H].

*3.1.5.2. 3-(3,4-Dimethoxyphenyl)-1H-pyrazole-5-carbaldehyde (**11b**).* 3-(3,4-Dimethoxyphenyl)-1*H*-pyrazole-5-carbaldehyde **11b** was prepared using above method by the addition of (3-(3,4-dimethoxyphenyl)-1*H*-pyrazol-5-yl)methanol **10b** (2.34 g, 10 mmol) IBX (3.36 g, 1.2 mmol). Yellow colored solid; (1.85 g, yield 82%): R_f = 0.4 (40% ethyl acetate/hexane); ^{1}H NMR (300 MHz, $CDCl_3$); δ ppm; δ 3.87 (s, 3H, −OC**H**$_3$), 3.91 (s, 3H, −OC**H**$_3$), 6.93–7.04 (m, 1H, Ar**H**), 7.27–7.47 (m, 2H, Ar**H**), 7.86–8.10 (m, 1H, Ar**H**), 9.93 (s, 1H, C**H**O) ppm; MS (ESI) *m*/*z* 233 [M + H].

*3.1.5.3. 3-(3,4,5-Trimethoxyphenyl)-1H-pyrazole-5-carbaldehyde (**11c**).* 3-(3,4,5-Trimethoxyphenyl)-1*H*-pyrazole-5-carbaldehyde **11c** was prepared using above method by the addition of (3-(3,4,5-trimethoxyphenyl)-1*H*-pyrazol-5-yl)methanol **10c** (2.64 g, 10 mmol) IBX (3.36 g, 1.2 mmol). Yellow colored solid; (2.09 g, yield 80%): R_f = 0.3 (40% ethyl acetate/hexane); ^{1}H NMR (400 MHz, $CDCl_3$); δ 3.82 (s, 3H, −OC**H**$_3$), 3.92 (s, 6H, −OC**H**$_3$), 6.85–7.25 (m, 3H, Ar**H**), 9.96 (s, 1H, C**H**O) ppm; MS (ESI) *m*/*z* 263 [M + H].

*3.1.5.4. 3-(Benzo[d][1,3]dioxol-5-yl)-1H-pyrazole-5-carbaldehyde (**11d**).* 3-(Benzo[*d*][1,3]dioxol-5-yl)-1*H*-pyrazole-5-carbaldehyde **11d** was prepared using above method by the addition of (3-(benzo[*d*][1,3]dioxol-5-yl)-1*H*-pyrazol-5-yl)methanol **10d** (2.18 g, 10 mmol) IBX (3.36 g, 1.2 mmol). Yellow colored solid (1.83 g, yield 85%): R_f = 0.3 (40% ethyl acetate/hexane); ^{1}H NMR (300 MHz, $CDCl_3$); δ 6.03 (s, 2H, −OC**H**$_2$O), 7.35–7.45 (m, 1H, Ar**H**), 7.87–7.94 (m, 2H, Ar**H**), 8.10–8.17 (m, 1H, Ar**H**), 10.2 (s, 1H, C**H**O ppm); MS (ESI) *m*/*z* 217 [M + H].

*3.1.6. Synthesis of (Z)-3-((3-phenyl-1H-pyrazol-5-yl)methylene) indolin-2-one analogs **12**(**a**–**u**)*

To the 3-subtitutedphenyl-1*H*-pyrazole-5-carbaldehydes **11**(**a**–**d**) prepared in the above step was added corresponding substituted oxindoles and catalytic amount of piperdine (1.0 ml) in ethanol. Heated the reaction mixture to reflux for 4 h at 85 °C. The solid compounds obtained in the reaction vessel were filtered and washed with ethanol for 4–5 times. After complete air drying the final compounds (*Z*)-3-((3-phenyl-1*H*-pyrazol-5-yl)methylene) indolin-2-one analogs **12**(**a**–**u**) were obtained as pure solids (yield 75–80%).

*3.1.6.1. (Z)-3-((3-(4-Methoxyphenyl)-1H-pyrazol-5-yl)methylene) indolin-2-one (**12a**).* This compound was prepared using the procedure described above by the addition of 3-(4-methoxyphenyl)-1*H*-pyrazole-5-carbaldehyde **11a** (150 mg 0.0495 mmol) and indolin-2-one (0.065 g 0.0495 mmol). The compound obtained as saffron colored solid Yield: 117 mg (75%); mp: 190–192 °C; ^{1}H NMR (300 MHz, DMSO-d_6); δ 3.88 (s, 3H, −OC**H**$_3$), 7.05–7.09 (m, 4H, Ar**H**), 7.19–7.26 (m, 1H, Ar**H**), 7.42–7.49 (t, 1H, J_1 = 6.9 Hz, J_2 = 7.7 Hz, Ar**H**), 7.50 (s, 1H, −C**H**), 7.62 (d, 1H, *J* = 7.5 Hz, Ar**H**),

7.68 (d, 1H, J = 8.8 Hz, Ar**H**), 9.42 (brs, 2H, −N**H**); ^{13}C NMR (75 MHz, DMSO-d_6): δ 55.0, 109.3, 114.1, 114.3, 119.9, 120.9, 125.3, 126.5, 126.6, 129.1, 129.6, 140.3, 142.5, 159.0, 159.3, 169.3 ppm; IR (KBr) (ν_{max}/cm^{-1}): ν = 3136, 3058, 3003, 2963, 2832, 1897, 1673, 1598, 1516, 1344, 1252, 1204, 809 cm^{-1}; MS (ESI) m/z 318 [M + H]; HR-MS (ESI) m/z for $C_{19}H_{16}N_3O_2$ calculated m/z: 318.1237, found m/z: 318.1227.

*3.1.6.2. (Z)-5-Chloro-3-((3-(4-methoxyphenyl)-1H-pyrazol-5-yl) methylene)indolin-2-one (**12b**).* This compound was prepared using the procedure described above by the addition of 3-(4-methoxyphenyl)-1*H*-pyrazole-5-carbaldehyde **11a** (150 mg 0.0495 mmol) and 5-chloroindolin-2-one (82.9 mg 0.0495 mmol). The compound obtained as yellow colored solid Yield: 135 mg (78%); mp: 196–198 °C; ^{1}H NMR (300 MHz, DMSO-d_6); δ 3.85 (s, 3H, −OC**H**$_3$), 6.85–6.95 (m, 1H, Ar**H**), 7.00 (t, 2H, J = 9.0 Hz, Ar**H**), 7.24 (d, 1H, J_1 = 6.9 Hz, J_2 = 7.7 Hz, Ar**H**), 7.50 (s, 1H, Ar**H**), 7.62 (d, 1H, J = 7.5 Hz, Ar**H**), 7.68 (d, 1H, J = 8.1 Hz, Ar**H**), 7.55 (s, 1H, Ar**H**), 7.72–7.88 (m, 3H, Ar**H**), 8.1–8.63 (m, 1H, Ar**H**), 9.16 (brs, 1H, −N**H**), 10.6 (brs, 1H, −N**H**); ^{13}C NMR (75 MHz, DMSO-d_6): δ 55.1, 107.5, 110.5, 114.1, 114.4, 121.0, 123.4, 124.2, 125.0, 125.7, 126.6, 126.9, 129.0, 141.2, 159.0, 169.3 ppm; IR (KBr) (ν_{max}/cm^{-1}): ν = 3167, 3055, 2933, 1674, 1600, 1516, 1328, 1201, 1168, 1109, 949 cm^{-1}; MS (ESI) m/z 352 [M + H]; HR-MS (ESI) m/z for $C_{19}H_{15}O_2N_3$ calculated m/z: 352.0847, found m/z: 352.0841.

*3.1.6.3. (Z)-6-Chloro-3-((3-(4-methoxyphenyl)-1H-pyrazol-5-yl) methylene)indolin-2-one (**12c**).* This compound was prepared using the procedure described above by the addition of 3-(4-methoxyphenyl)-1*H*-pyrazole-5-carbaldehyde **11a** (150 mg 0.0495 mmol) and 6-chloroindolin-2-one (82.9 mg 0.0495 mmol). The compound obtained as pale yellow colored solid Yield: 132 mg (76%); mp: 190–192 °C; ^{1}H NMR (300 MHz, DMSO-d_6); δ 3.83 (s, 3H, −OC**H**$_3$), 6.83–7.08 (m, 4H, Ar**H**), 7.59 (d, 1H, J = 8.1 Hz, Ar**H**), 7.65 (s, 1H, Ar**H**), 7.72 (d, 1H, J = 8.1 Hz, Ar**H**), 7.78 (d, 1H, J = 8.4 Hz, Ar**H**), 7.91–7.96 (m, 1H, Ar**H**), 9.03 (brs, 1H, −N**H**), 10.51 (brs, 1H, −N**H**); ^{13}C NMR (75 MHz, DMSO-d_6): δ 55.1, 109.3, 114.1, 114.4, 120.6, 126.28, 126.5, 126.6, 127.4, 133.7, 143.8, 159.3, 169.3 ppm; IR (KBr) (ν_{max}/cm^{-1}): ν = 3155, 3027, 2966, 2933, 2836, 1676, 1593, 1515, 1455, 1344, 1251, 1205, 1175, 1063, 1025 cm^{-1}; MS (ESI) m/z 352 [M + H]; HR-MS (ESI) m/z for $C_{19}H_{15}O_2N_3$ calculated m/z: 352.0847, found m/z: 352.0844.

*3.1.6.4. (Z)-5-Methoxy-3-((3-(4-methoxyphenyl)-1H-pyrazol-5-yl) methylene)indolin-2-one (**12d**).* This compound was prepared using the procedure described above by the addition of 3-(4-methoxyphenyl)-1*H*-pyrazole-5-carbaldehyde **11a** (150 mg 0.0495 mmol) and 5-methoxyindolin-2-one (80 mg 0.0495 mmol). The compound obtained as saffron colored solid Yield: 137 mg (80%); mp: 208–210 °C; ^{1}H NMR (300 MHz, DMSO-d_6); δ 3.87 (s, 3H, −OC**H**$_3$), 3.79 (s, 3H, −OC**H**$_3$), 6.73–6.79 (m, 2H, Ar**H**), 7.01 (d, 2H, J = 8.4 Hz, Ar**H**), 7.06–7.30 (m, 1H, Ar**H**), 7.42 (s, 1H, =C**H**), 7.69–7.83 (m, 2H, Ar**H**), 7.85 (s, 1H, Ar**H**), 8.82 (brs, 1H, −N**H**), 10.9 (brs, 1H, −N**H**); ^{13}C NMR (75 MHz, DMSO-d_6): δ 55.2, 55.5, 105.9, 109.4, 114.2, 114.4, 122.7, 125.9, 126.7, 126.6, 134.0, 136.1, 154.4, 155.0, 159.1, 159.4, 169.5 ppm; IR (KBr) (ν_{max}/cm^{-1}): ν = 3448, 3120, 3069, 2995, 2956, 2828, 1677, 1610, 1516, 1337, 1247, 1207, 1167 cm^{-1}; MS (ESI) m/z 352 [M + H]; HR-MS (ESI) m/z for $C_{19}H_{15}O_2N_3$ calculated m/z: 352.0847, found m/z: 352.0844.

*3.1.6.5. (Z)-3-((3-(4-Methoxyphenyl)-1H-pyrazol-5-yl)methylene)-5-nitroindolin-2-one (**12e**).* This compound was prepared using the procedure described above by the addition of 3-(4-methoxyphenyl)-1*H*-pyrazole-5-carbaldehyde **11a** (150 mg 0.0495 mmol) and 5-nitroindolin-2-one (88 mg 0.0495 mmol). The compound obtained as brown red colored solid Yield: 138 mg (77%); mp: 218–220 °C; ^{1}H NMR (300 MHz, DMSO-d_6); δ 3.80 (s, 3H, −OC**H**$_3$), 7.01–7.11 (m, 3H, Ar**H**), 7.20 (s, 1H, Ar**H**), 7.63 (s, 1H, =C**H**), 7.78 (d, 1H, J = 8.6 Hz, Ar**H**), 8.17–8.28 (m, 2H, Ar**H**), 10.04 (brs, 1H, −N**H**); ^{13}C NMR (75 MHz, DMSO-d_6): δ 55.2, 107.9, 109.4, 114.5, 121.7, 121, 122.1, 123.1, 126.3, 126.8, 128.6, 142.0, 148.1, 159.5, 169.8 ppm; IR (KBr) (ν_{max}/cm^{-1}): ν = 3293, 3142, 2932, 2834, 1697, 1613, 1518, 1332, 1250, 1178, 1125 cm^{-1}; MS (ESI) m/z 363 [M + H]; HR-MS (ESI) m/z for $C_{19}H_{15}O_4N_4$ calculated m/z: 363.1087, found m/z: 363.1082.

*3.1.6.6. (Z)-5-Chloro-3-((3-(3,4,5-Trimethoxyphenyl)-1H-pyrazol-5-l)methylene)indolin-2-one (**12f**).* This compound was prepared using the procedure described above by the addition of 3-(3, 4, 5-trimethoxyphenyl)-1*H*-pyrazole-5-carbaldehyde **11c** (150 mg 0.0572 mmol) and 5-chloroindolin-2-one (95 mg 0.0572 mmol). The compound obtained as yellow colored crystal Yield: 192 mg (82%); mp: 198–200 °C; ^{1}H NMR (400 MHz, DMSO-d_6); δ 3.69 (s, 3H, −OC**H**$_3$), 3.86 (s, 6H, −OC**H**$_3$), 6.90 (d, 1H, J = 8.3 Hz, Ar**H**), 7.17 (s, 2H, =C**H**, Ar**H**), 7.27 (s, 1H, Ar**H**), 7.30–7.39 (m, 1H, Ar**H**), 7.50 (s, 1H, Ar**H**), 7.86–7.96 (m, 1H Ar**H**), 9.18 (brs, 1H, −N**H**), 10.71 (brs, 1H, −N**H**); ^{13}C NMR (75 MHz, DMSO-d_6): δ 55.9, 60.1, 102.9, 108.3, 110.7, 120.1, 123.4, 124.4, 125.2, 126.9, 126. 129.2, 137.7, 141.2, 153.3, 169.2 ppm; IR (KBr) (ν_{max}/cm^{-1}): ν = 3115, 2947, 2832, 1683, 1612, 1587, 1545, 1513, 1463, 1427, 1377, 1346, 1237, 1178, 1132, 1070 cm^{-1}; MS (ESI) m/z 412 [M + H]; HR-MS (ESI) m/z for $C_{21}H_{19}O_4N_3Cl$ calculated m/z: 412.1058, found m/z: 412.1044.

*3.1.6.7. (Z)-3-((3-(3,4,5-Trimethoxyphenyl)-1H-pyrazol-5-yl)methylene)indolin-2-one (**12g**).* This compound was prepared using the procedure described above by the addition of 3-(3,4,5-trimethoxyphenyl)-1*H*-pyrazole-5-carbaldehyde **11c** (150 mg 0.0572 mmol) and indolin-2-one (76 mg 0.0572 mmol). The compound obtained as brown colored solid Yield: 168 mg (78%); mp: 208–210 °C; ^{1}H NMR (300 MHz, DMSO-d_6); δ 3.72 (s, 3H, −OC**H**$_3$), 3.88 (s, 6H, −OC**H**$_3$), 6.86–7.01 (m, 1H, Ar**H**), 7.15 (s, 2H, =C**H**, Ar**H**), 7.22–7.32 (m, 1H, Ar**H**), 7.47 (s, 1H, Ar**H**), 7.67–7.82 (t, 1H, J = 7.5 Hz, Ar**H**), 8.23 (m, 1H, Ar**H**), 9.18 (s, 1H, −Ar**H**), 10.54 (brs, 1H, −N**H**), 11.12 (brs, 1H, −N**H**); ^{13}C NMR (75 MHz, DMSO-d_6): δ 54.2, 58.2, 100.9, 101.5, 105.9, 107.6, 108.2, 118.1, 119.1, 119.8, 123.8, 124.2, 127.3, 127.8, 138.5, 140.7, 151.3, 151.5, 166.7, 167.7 ppm; IR (KBr) (ν_{max}/cm^{-1}): ν = 3114, 3054, 2935, 2827, 1677, 1600, 1544, 1513, 1471, 1349, 1127, 1075, 1009 cm^{-1}; MS (ESI) m/z 378 [M + H]; HR-MS (ESI) m/z for $C_{21}H_{20}O_4N_3$ calculated m/z: 378.14483, found m/z: 378.1441.

*3.1.6.8. (Z)-3-((3-(3,4-Dimethoxyphenyl)-1H-pyrazol-5-yl)methylene)indolin-2-one (**12h**).* This compound was prepared using the procedure described above by the addition of 3-(3, 4-dimethoxyphenyl)-1*H*-pyrazole-5-carbaldehyde **11b** (150 mg 0.0659 mmol) and indolin-2-one (86 mg 0.0659 mmol). The compound obtained as yellow colored solid Yield: 182 mg (80%); mp: 196–198 °C; ^{1}H NMR (300 MHz, DMSO-d_6); δ 3.82 (s, 3H, −OC**H**$_3$), 3.87 (s, 3H, −OC**H**$_3$), 6.87–7.13 (m, 3H, Ar**H**), 7.25 (s, 1H, =C**H**), 7.34–7.46 (m, 2H, Ar**H**), 7.73 (t, 1H, J = 7.5 Hz, Ar**H**), 8.24 (s, 1H, Ar**H**), 9.03 (s, 1H, −N**H**), 11.09 (brs, 1H, −N**H**); ^{13}C NMR (75 MHz, DMSO-d_6): δ 55.5, 55.6, 108.7, 108.9, 109.4, 111.8, 111.9, 129.21, 129.6, 148.7, 148.9, 149.0, 169.6 ppm; IR (KBr) (ν_{max}/cm^{-1}): ν = 3163, 3024, 2836, 1678, 1604, 1516, 1471, 1423, 1380, 1348, 1308, 1266, 1228, 1201, 1153, 1020 cm^{-1}; MS (ESI) m/z 348 [M + H]; HR-MS (ESI) m/z for $C_{20}H_{18}O_3N_3$ calculated m/z: 348.13427, found m/z: 348.13318.

*3.1.6.9. (Z)-5-Chloro-3-((3-(3,4-dimethoxyphenyl)-1H-pyrazol-5-yl) methylene)indolin-2-one (**12i**).* This compound was prepared using the procedure described above by the addition of 3-(3,4-

dimethoxyphenyl)-1*H*-pyrazole-5-carbaldehyde **11b** (150 mg 0.0659 mmol) and 5-chloroindolin-2-one (110 mg 0.0659 mmol). The compound obtained as yellow colored solid Yield: 193 mg (77%); mp: 198–199 °C; ^{1}H NMR (500 MHz, DMSO-d_6); δ 3.80 (s, 3H, −OC**H**$_3$), 3.84 (s, 3H, −OC**H**$_3$), 6.88 (d, 1H, J = 8.3 Hz, Ar**H**), 7.01 (d, 1H, J = 8.4 Hz, Ar**H**), 7.19 (s, 1H, =C**H**), 7.26–7.42 (m, 2H, Ar**H**), 7.46 (s, 1H, Ar**H**), 7.52 (s, 1H Ar**H**), 7.85–7.99 (m, 1H, Ar**H**), 9.21 (brs, 1H, −N**H**), 10.7 (brs, 1H, −N**H**); ^{13}C NMR (75 MHz, DMSO-d_6): δ 55.5, 55.6, 107.7, 108.7, 108.9, 110.6, 117.9, 112, 124.2, 125.1, 125.8, 127.0, 129.1, 141.2, 143.5, 147.3, 148.9, 149, 169.2 ppm; IR (KBr) (ν_{max}/cm^{-1}): ν = 3118, 2955, 2829, 1680, 1609, 1522, 1437, 1382, 1343, 1263, 1234, 1157, 1064, 1026 cm^{-1}; MS (ESI) m/z 348 [M + H]; HR-MS (ESI) m/z for $C_{20}H_{17}O_3N_3Cl$ calculated m/z: 382.0953, found m/z: 382.0950.

*3.1.6.10. (Z)-6-Chloro-3-((3-(3,4-Dimethoxyphenyl)-1H-pyrazol-5-yl)methylene)indolin-2-one (**12j**).* This compound was prepared using the procedure described above by the addition of 3-(3,4-dimethoxyphenyl)-1*H*-pyrazole-5-carbaldehyde **11b** (150 mg 0.0659 mmol) and 6-chloroindolin-2-one (110 mg 0.0659 mmol). The compound obtained as yellow colored solid Yield: 191 mg (76%); mp: 196–198 °C; ^{1}H NMR (500 MHz, DMSO-d_6); δ 3.80 (s, 3H, −OC**H**$_3$), 3.85 (s, 3H, −OC**H**$_3$), 6.88 (m, 1H, Ar**H**), 7.0–7.14 (m, 2H, Ar**H**), 7.17 (s, 1H, =C**H**), 7.36 (d, 1H, J = 8.1 Hz Ar**H**), 7.42 (s, 1H, Ar**H**), 7.48 (s, 1H Ar**H**), 7.78–7.88 (m, 1H, Ar**H**), 9.1 (brs, 1H, −N**H**), 10.7 (brs, 1H, −N**H**); ^{13}C NMR (75 MHz, DMSO-d_6): δ 55.4, 55.5, 107.2, 109.0, 109.3, 112.0, 120.5, 124.0, 126.2, 127.4, 133.6, 143.4, 143.8, 147.2, 148.9, 169.3 ppm; IR (KBr) (ν_{max}/cm^{-1}): ν = 3120, 2951, 2829, 1680, 1605, 1522, 1437, 1382, 1343, 1250, 1234, 1157, 1064, 1026 cm^{-1}; MS (ESI) m/z 348 [M + H]; HR-MS (ESI) m/z for $C_{20}H_{17}O_3N_3Cl$ calculated m/z: 382.0953, found m/z: 382.0950.

*3.1.6.11. (Z)-3-((3-(3,4-Dimethoxyphenyl)-1H-pyrazol-5-yl)methylene)-5-methoxyindolin-2-one (**12k**).* This compound was prepared using the procedure described above by the addition of 3-(3,4-dimethoxyphenyl)-1*H*-pyrazole-5-carbaldehyde **11b** (150 mg, 0.0659 mmol) and 5-methoxyindolin-2-one (107 mg, 0.0659 mmol). The compound obtained as saffron colored solid Yield: 196 mg (79%); mp: 192–195 °C; ^{1}H NMR (300 MHz, DMSO-d_6); δ 3.77 (s, 3H, −OC**H**$_3$), 3.79 (s, 3H, −OC**H**$_3$), 3.84 (s, 3H, −OC**H**$_3$), 6.70–6.93 (m, 1H, Ar**H**), 6.98–7.20 (m, 2H, =C**H**, Ar**H**), 7.31–7.52 (m, 3H, Ar**H**), 7.85 (s, 1H, Ar**H**), 8.84 (s, 1H, Ar**H**), 10.3 (brs, 1H, −N**H**), 10.9 (brs, 1H, −N**H**); ^{13}C NMR (75 MHz, DMSO-d_6): δ 55.4, 105.9, 107.2, 109.9, 108.9, 108.7, 111.9, 112.0, 114.5, 117.8, 122.7, 125.9, 134.11, 136.2, 149.0, 154.4, 155.0, 169.5 ppm; IR (KBr) (ν_{max}/cm^{-1}): ν = 3121, 3000, 2912, 2839, 1676, 1610, 1517, 1479, 1435, 1381, 1336, 1302, 1274, 1205, 1230, 1165, 1131, 1062 cm^{-1}; MS (ESI) m/z 378 [M + H]; HR-MS (ESI) m/z for $C_{21}H_{20}O_4N_3$ calculated m/z: 378.14483, found m/z: 378.14395.

*3.1.6.12. (Z)-3-((3-(3,4-Dimethoxyphenyl)-1H-pyrazol-5-yl)methylene)-5-nitroindolin-2-one (**12l**).* This compound was prepared using the procedure described above by the addition of 3-(3,4-dimethoxyphenyl)-1*H*-pyrazole-5-carbaldehyde **11b** (150 mg, 0.0659 mmol) and 5-nitroindolin-2-one (117 mg, 0.0659 mmol). The compound obtained as yellow colored solid Yield: 193 mg (75%); mp: 174–176 °C; ^{1}H NMR (300 MHz, DMSO-d_6); δ 3.80 (s, 3H, −OC**H**$_3$), 3.86 (s, 3H, −OC**H**$_3$), 7.06 (d, 3H, J = 8.6 Hz Ar**H**), 7.24 (s, 1H, =C**H**), 7.40 (d, 1H, J = 8.3 Hz Ar**H**), 7.45 (s, 1H, Ar**H**), 7.63 (s, 1H Ar**H**), 8.12–8.34 (m, 1H, Ar**H**), 10.07 (brs, 1H, −N**H**), 11.2 (brs, 1H, −N**H**); ^{13}C NMR (75 MHz, DMSO-d_6): δ 55.4, 55.5, 108.9, 112.0, 118.0, 120.9, 121.9, 122.1, 123.1, 126.3, 128.6, 141.9, 143.7, 147.1, 148.1, 149.0, 169.7 ppm; IR (KBr) (ν_{max}/cm^{-1}): ν = 3166, 3011, 2908, 1689, 1605, 1523, 1467, 1434, 1341, 1385, 1263, 1240, 1197, 1161, 1141, 1076, 1029 cm^{-1}; MS (ESI) m/z 393 [M + H]; HR-MS (ESI) m/z for $C_{20}H_{17}O_5N_4$ calculated m/z: 393.11935, found m/z: 393.11945.

*3.1.6.13. (Z)-6-Chloro-3-((3-(3,4,5-trimethoxyphenyl)-1H-pyrazol-5-yl)methylene)indolin-2-one (**12m**).* This compound was prepared using the procedure described above by the addition of 3-(3,4,5-trimethoxyphenyl)-1*H*-pyrazole-5-carbaldehyde **11c** (150 mg 0.0572 mmol) and 6-chloroindolin-2-one (95 mg 0.0572 mmol). The compound obtained as yellow colored solid Yield: 183 mg (75%); mp: 184–186 °C; ^{1}H NMR (500 MHz, DMSO-d_6); δ 3.69 (s, 3H, −OC**H**$_3$), 3.84 (s, 6H, −OC**H**$_3$), 6.82–6.99 (m, 1H, Ar**H**), 7.03–7.12 (m, 1H, Ar**H**), 7.15 (s, 1H, =C**H**), 7.25 (s, 1H, Ar**H**), 7.48 (s, 1H, Ar**H**), 7.70–7.94 (m, 1H, Ar**H**), 9.09 (d, 1H, J = 8.3 Hz Ar**H**), 10.7 (brs, 1H, −N**H**), 11.2 (brs, 1H, −N**H**); ^{13}C NMR (75 MHz, DMSO-d_6): δ 55.8, 56.0, 60.0, 102.6, 102.8, 108.0, 109.3, 110.0, 120.6, 121.5, 121.7, 124.1, 124.3, 126.2, 127.5, 128.3, 133.7, 139.2, 141.4, 143.4, 147.43, 151.5, 153.3, 153.1, 168.6, 169.4 ppm; IR (KBr) (ν_{max}/cm^{-1}): ν = 3115, 2947, 2832, 1683, 1612, 1587, 1545, 1513, 1463, 1427, 1377, 1346, 1236, 1179, 1132, 1070, 1039 cm^{-1}; MS (ESI) m/z 412 [M + H]; HR-MS (ESI) m/z for $C_{21}H_{19}O_4N_3Cl$ calculated m/z: 412.1058, found m/z: 412.1065.

*3.1.6.14. (Z)-5-Methoxy-3-((3-(3,4,5-trimethoxyphenyl)-1H-pyrazol-5-yl)methylene)indolin-2-one (**12n**).* This compound was prepared using the procedure described above by the addition of 3-(3,4,5-trimethoxyphenyl)-1*H*-pyrazole-5-carbaldehyde **11c** (150 mg, 0.0572 mmol) and 5-methoxyindolin-2-one (93 mg, 0.0572 mmol). The compound obtained as saffron colored solid Yield: 195 mg (81%); mp: 208–210 °C; ^{1}H NMR (300 MHz, DMSO-d_6); δ 3.70 (s, 3H, −OC**H**$_3$), 3.77 (s, 3H, −OC**H**$_3$), 3.87 (s, 6H, −OC**H**$_3$), 6.72–6.94 (m, 1H, Ar**H**), 7.14 (s, 1H, Ar**H**), 7.16 (s, 1H, =C**H**), 7.43 (s, 1H, Ar**H**), 7.85 (s, 1H, Ar**H**), 10.8 (brs, 1H, −N**H**), 14.45 (brs, 1H, −N**H**); ^{13}C NMR (75 MHz, DMSO-d_6): δ 55.5, 56.0, 60.0, 102.7, 102.9, 106.0, 109.4, 114.6, 115.1, 122.5, 126.0, 125.9, 134.0, 136.2, 137.6, 153.1, 154.3, 154.9, 169.4 ppm; IR (KBr) (ν_{max}/cm^{-1}): ν = 3121, 2942, 2837, 1678, 1592, 1544, 1511, 1481, 1430, 1383, 1339, 1302, 1269, 1238, 1201, 1171, 1124, 1085 cm^{-1}; MS (ESI) m/z 408 [M + H]; HR-MS (ESI) m/z for $C_{22}H_{22}O_5N_3$ calculated m/z: 408.15540, found m/z: 408.15567.

*3.1.6.15. (Z)-5-Nitro-3-((3-(3,4,5-trimethoxyphenyl)-1H-pyrazol-5-yl)methylene)indolin-2-one (**12o**).* This compound was prepared using the procedure described above by the addition of 3-(3,4,5-trimethoxyphenyl)-1*H*-pyrazole-5-carbaldehyde **11c** (150 mg, 0.0572 mmol) and 5-nitroindolin-2-one (101 mg, 0.0572 mmol). The compound obtained as light yellow colored solid. Yield: 190 mg (79%); mp: 203–205 °C; ^{1}H NMR (300 MHz, DMSO-d_6); δ 3.86 (s, 3H, −OC**H**$_3$), 6.69–6.94 (m, 2H, Ar**H**), 7.14 (d, 1H, Ar**H**), 7.25 (s, 1H, =C**H**), 7.43 (s, 1H, Ar**H**), 7.85 (s, 1H, Ar**H**), 10.8 (brs, 1H, −N**H**), 14.45 (brs, 1H, −N**H**); ^{13}C NMR (75 MHz, DMSO-d_6): δ 56.0, 60.0, 102.7, 102.9, 108.7, 109.2, 121.7, 122.0, 123.2, 123.7, 126.2, 128.3, 137.7, 141.9, 143.7, 147.0, 148.1, 153.2, 169.6 ppm; IR (KBr) (ν_{max}/cm^{-1}): ν = 3121, 2942, 2837, 1678, 1592, 1544, 1511, 1481, 1430, 1383, 1339, 1302, 1269, 1238, 1201, 1171, 1124, 1085 cm^{-1}; MS (ESI) m/z 423 [M + H]; HR-MS (ESI) m/z for $C_{21}H_{19}O_5N_4$ calculated m/z: 423.12230, found m/z: 423.12240.

*3.1.6.16. (Z)-3-((3-(Benzo[d][1,3]dioxol-5-yl)-1H-pyrazol-5-yl)methylene)-5-nitroindolin-2-one (**12p**).* This compound was prepared using the procedure described above by the addition of 3-(benzo[*d*][1,3]dioxol-5-yl)-1*H*-pyrazole-5-carbaldehyde **11d** (150 mg, 0.0694 mmol) and 5-nitroindolin-2-one (123 mg, 0.0694 mmol). The compound obtained as light yellow colored solid Yield: 195 mg (75%); mp: 196–198 °C; ^{1}H NMR (500 MHz, DMSO-d_6); δ 6.11 (s, 2H, −OC**H**$_2$O), 6.97–7.16 (m, 2H, Ar**H**), 7.23 (s, 1H, =C**H**), 7.38 (d, 1H, J = 8.1 Hz Ar**H**), 7.45 (s, 1H, Ar**H**), 7.61 (s, 1H, Ar**H**), 8.14–8.34 (m, 1H, Ar**H**), 10.0 (s, 1H, Ar**H**)11.29 (brs, 1H, −N**H**), 14.13 (brs, 1H, −N**H**); ^{13}C NMR (75 MHz, DMSO-d_6): δ 101.3, 105.7, 108.4, 108.8, 109.3, 119.3, 121.7, 122.1, 122.4, 123.1, 126.3, 128.4, 141.9, 147.8, 148.1, 147.4, 147.0, 169.7 ppm; IR (KBr) (ν_{max}/cm^{-1}): ν = 3117, 2917, 1684, 1620, 1549, 1515, 1461, 1416, 1337, 1244, 1187, 1127, 1079, 1039 cm^{-1}; MS (ESI)

m/*z* 377 [M + H]; HR-MS (ESI) *m*/*z* for $C_{19}H_{13}N_4O_5$ calculated *m*/*z*: 377.32440, found *m*/*z*: 377.32410.

*3.1.6.17. (Z)-3-((3-(Benzo[d][1,3]dioxol-5-yl)-1H-pyrazol-5-yl)methylene)-6-chloroindolin-2-one (**12q**).* This compound was prepared using the procedure described above by the addition of 3-(benzo[*d*][1,3]dioxol-5-yl)-1*H*-pyrazole-5-carbaldehyde **11d** (150 mg, 0.0694 mmol) and 6-chloroindolin-2-one (115 mg 0.0694 mmol). The compound obtained as light yellow colored solid Yield: 202 mg (80%); mp: 210–212 °C; ^{1}H NMR (300 MHz, DMSO-d_6); δ 6.11 (s, 2H, −OC**H**$_2$O), 6.80–7.11 (m, 3H, Ar**H**), 7.25–7.39 (m, 2H, Ar**H**), 7.45 (s, 1H, =C**H**), 7.65–7.85 (m, 3H, Ar**H**), 8.26 (s, 1H, Ar**H**), 8.90 (brs, 1H, −N**H**); ^{13}C NMR (75 MHz, DMSO-d_6): δ 100.9, 101.1, 105.4, 105.6, 108.3, 108.5, 109.2, 118.8, 119.0, 120.4, 124.1, 133.7, 141.3, 143.7, 146.9, 147.3, 147.5, 147.7, 169.3 ppm; IR (KBr) (ν_{max}/cm^{-1}): ν = 3160, 3092, 1697, 1614, 1512, 1471, 1439, 1381, 1312, 1240, 1199, 1168, 1057 cm^{-1}; MS (ESI) *m*/*z* 366 [M + H]; HR-MS (ESI) *m*/*z* for $C_{19}H_{13}ClN_3O_3$ calculated *m*/*z*: 366.06513, found *m*/*z*: 366.06509.

*3.1.6.18. (Z)-3-((3-(Benzo[d][1,3]dioxol-5-yl)-1H-pyrazol-5-yl)methylene)-5-chloroindolin-2-one (**12r**).* This compound was prepared using the procedure described above by the addition of 3-(benzo[*d*][1,3]dioxol-5-yl)-1*H*-pyrazole-5-carbaldehyde **11d** (150 mg 0.0694 mmol) and 6-chloroindolin-2-one (115 mg 0.0694 mmol). The compound obtained as yellow colored solid Yield: 202 mg (80%); mp: 208–210 °C; ^{1}H NMR (300 MHz, DMSO-d_6); δ 6.10 (s, 2H, −OC**H**$_2$O), 6.80–7.11 (m, 2H, Ar**H**), 7.20–7.32 (m, 3H, Ar**H**), 7.35 (s, 1H, =C**H**), 7.51–7.74 (m, 2H, Ar**H**), 7.81 (s, 1H, Ar**H**), 8.46 (s, 1H, Ar**H**), 9.21 (brs, 1H, −N**H**); ^{13}C NMR (75 MHz, DMSO-d_6): δ 100.9, 101.1, 105.4, 105.6, 108.3, 108.5, 109.2, 118.8, 119.0, 120.4, 124.1, 133.7, 141.3, 143.7, 146.9, 147.3, 147.5, 147.7, 169.3 ppm; IR (KBr) (ν_{max}/cm^{-1}): ν = 3160, 3092, 1697, 1614, 1512, 1471, 1439, 1381, 1312, 1240, 1199, 1168, 1057 cm^{-1}; MS (ESI) *m*/*z* 366 [M + H]; HR-MS (ESI) *m*/*z* for $C_{19}H_{13}ClN_3O_3$ calculated *m*/*z*: 366.06513, found *m*/*z*: 366.06509.

*3.1.6.19. (Z)-3-((3-(Benzo[d][1,3]dioxol-5-yl)-1H-pyrazol-5-yl)methylene)-5-methoxyindolin-2-one (**12s**).* This compound was prepared using the procedure described above by the addition of 3-(benzo[*d*][1,3]dioxol-5-yl)-1*H*-pyrazole-5-carbaldehyde **11d** (150 mg, 0.0694 mmol) and 5-methoxyindolin-2-one (113 mg, 0.0694 mmol). The compound obtained as yellow colored solid Yield: 207 mg (83%); mp: 205–207 °C; ^{1}H NMR (500 MHz, DMSO-d_6); δ 3.86 (s, 3H, −OC**H**$_3$), 6.08 (s, 2H, −OC**H**$_2$O), 6.70–6.94 (m, 2H, Ar**H**), 6.93–7.14 (m, 1H, Ar**H**), 7.16 (d, 1H, *J* = 11.8, Ar**H**), 7.27–7.54 (m, 3H, =C**H**, Ar**H**), 7.86 (s, 1H, Ar**H**), 8.85 (brs, 1H, N**H**), 10.98 (brs, 1H, −N**H**); ^{13}C NMR (75 MHz, DMSO-d_6): δ 53.5, 99.4, 103.7, 103.9, 106.8, 108.7, 111.9, 112.0, 114.5, 117.8, 122.7, 134.11, 136.2, 147.5, 149.0, 154.4, 155.0, 169.5 ppm; IR (KBr) (ν_{max}/cm^{-1}): ν = 3445, 3120, 3002, 2825, 2722, 1678, 1614, 1545, 1511, 1466, 1437, 1397, 1333, 1273, 1241, 1205, 1164 cm^{-1}; MS (ESI) *m*/*z* 362 [M + H]; HR-MS (ESI) *m*/*z* for $C_{21}H_{15}N_3O_4$ calculated *m*/*z*: 362.11034, found *m*/*z*: 362.11060.

*3.1.6.20. (Z)-3-((3-(Benzo[d][1,3]dioxol-5-yl)-1H-pyrazol-5-yl)methylene)-5-fluoroindolin-2-one (**12t**).* This compound was prepared using the procedure described above by the addition of 3-(benzo[*d*][1,3]dioxol-5-yl)-1*H*-pyrazole-5-carbaldehyde **11d** (150 mg 0.0694 mmol) and 5-fluoroindolin-2-one (104 mg 0.0694 mmol). The compound obtained as yellow colored solid. Yield: 176 mg (73%); mp: 185–187 °C; ^{1}H NMR (500 MHz, DMSO-d_6); δ 6.08 (s, 2H, −OC**H**$_2$O), 6.74–7.22 (m, 4H, Ar**H**), 7.25–7.91 (m, 3H, Ar**H**, =C**H**), 8.24 (s, 1H, Ar**H**), 10.52 (brs, 1H, N**H**), 11.11 (brs, 1H, −N**H**); ^{13}C NMR (75 MHz, DMSO-d_6): δ 85.0, 99.49, 103.9, 106.8, 117.2, 117.4, 124.9, 132.0, 145.7, 146.1, 167.9 ppm; IR (KBr) (ν_{max}/cm^{-1}): ν = 3127, 1858, 1680, 1611, 1545, 1511, 1466, 1435, 1396, 1335, 1243, 1198, 1165, 1110, 1041 cm^{-1}; MS (ESI) *m*/*z* 362 [M + H]; HR-MS (ESI) *m*/*z* for $C_{21}H_{15}N_3FO_4$ calculated *m*/*z*: 362.11034, found *m*/*z*: 362.11060.

*3.1.6.21. (Z)-5-Fluoro-3-((3-(4-methoxyphenyl)-1H-pyrazol-5-yl)methylene)indolin-2-one (**12u**).* This compound was prepared using the procedure described above by the addition of 3-(4-methoxyphenyl)-1*H*-pyrazole-5-carbaldehyde **11a** (150 mg 0.0495 mmol) and 5-fluoroindolin-2-one (74 mg 0.0694 mmol). The compound obtained as yellow colored solid Yield: 124 mg (75%); mp: 190–192 °C; ^{1}H NMR (500 MHz, DMSO-d_6); δ 3.86 (s, 3H, −OC**H**$_3$), 6.75–7.25 (m, 5H, Ar**H**), 7.55 (s, 1H, Ar**H**), 7.60–7.95 (m, 2H, Ar**H**, =C**H**), 8.04 (s, 1H, Ar**H**), 10.98 (brs, 1H, N**H**), 13.88 (brs, 1H, −N**H**); ^{13}C NMR (75 MHz, DMSO-d_6): δ 85.0, 99.49, 103.9, 106.8, 117.2, 117.4, 124.9, 132.0, 145.7, 146.1, 167.9 ppm; IR (KBr) (ν_{max}/cm^{-1}): ν = 3010, 2965, 2928, 2809, 2702, 1679, 1611, 1577, 1517, 1481, 1461, 1435, 1384, 1337, 1284, 1249, 1201, 1169, 1105, 1054, 1030 cm^{-1}; MS (ESI) *m*/*z* 336 [M + H]; HR-MS (ESI) *m*/*z* for $C_{19}H_{15}N_3O_2F$ calculated *m*/*z*: 336.11414, found *m*/*z*: 336.11414.

3.2. Cell cultures, maintenance and antiproliferative evaluation

All cell lines used in this study were purchased from the American Type Culture Collection (ATCC, United States). A549, MCF-7, and HeLa were grown in Dulbecco's modified Eagle's medium (containing 10% FBS in a humidified atmosphere of 5% CO_2 at 37 °C). DU145 cells were cultured in Eagle's minimal essential medium (MEM) containing non-essential amino acids, 1 mM sodium pyruvate, 10 mg/mL bovine insulin, and 10% FBS. Cells were trypsinized when sub-confluent from T25 flasks/60 mm dishes and seeded in 96-wel plates. The synthesized test compounds were evaluated for their *in vitro* antiproliferative in four different human cancer cell lines. A protocol of 48 h continuous drug exposure was used, and a MTT cell proliferation assay was used to estimate cell viability or growth. The cell lines were grown in their respective media containing 10% fetal bovine serum and were seeded into 96-well microtiter plates in 200 μL aliquots at plating densities depending on the doubling time of individual cell lines. The microtiter plates were incubated at 37 °C, 5% CO_2, 95% air, and 100% relative humidity for 24 h prior to addition of experimental drugs. Aliquots of 2 μL of the test compounds were added to the wells already containing 198 μL of cells, resulting in the required final drug concentrations. For each compound, four concentrations (1, 10, 100, and 1000 μM) were evaluated, and each was done in triplicate wells. Plates were incubated further for 48 h, and the assay was terminated by the addition of 10 μL of 5% MTT and incubated for 60 min at 37 °C. Later, the plates were air-dried. Bound stain was subsequently eluted with 100 μL of DMSO, and the absorbance was read on a multimode plate reader (Tecan M200) at a wavelength of 560 nm. Percent growth was calculated on a plate by plate basis for test wells relative to control wells. The above determinations were repeated thrice. The growth inhibitory effects of the compounds were analyzed by generating dose response curves as a plot of the percentage surviving cells versus compound concentration. The sensitivity of the cancer cells to the test compound was expressed in terms of IC_{50}, a value defined as the concentration of compound that produced 50% reduction as compared to the control absorbance. IC_{50} values are indicated as means ± SD of three independent experiments [28].

3.2.1. Analysis of cell cycle

HeLa cells in 60 mm dishes were incubated for 24 h in the presence or absence of test compounds **12b**, **12c** and **12d** at 5 μM or 10 μM concentrations. Cells were harvested with Trypsin–EDTA, fixed with ice-cold 70% ethanol at 4 °C for 30 min, ethanol was removed by centrifugation and cells were stained with 1 mL of DNA staining solution [0.2 mg of Propidium Iodide (PI), and 2 mg RNase

A] for 30 min as described earlier. The DNA contents of 20,000 events were measured by flow cytometer (BD FACSCanto II). Histograms were analyzed using FCS express 4 plus [28].

3.2.2. Tubulin polymerization assay

An *in vitro* assay for monitoring the time-dependent polymerization of tubulin to microtubules was performed employing a fluorescence-based tubulin polymerization assay kit (BK011, Cytoskeleton, Inc.) according to the manufacturer's protocol. The reaction mixture in a final volume of 10 μl in PEM buffer (80 mM PIPES, 0.5 mM EGTA, 2 mM $MgCl_2$, pH 6.9) in 384 well plates contained 2 mg/mL bovine brain tubulin, 10 μM fluorescent reporter, 1 mM GTP in the presence or absence of test compounds at 37 °C. Tubulin polymerization was followed by monitoring the fluorescence enhancement due to the incorporation of a fluorescence reporter into microtubules as polymerization proceeds. Fluorescence emission at 420 nm (excitation wavelength is 360 nm) was measured for 1 h at 1 min intervals in a multimode plate reader (Tecan M200). To determine the IC_{50} values of the compounds against tubulin polymerization, the compounds were pre-incubated with tubulin at varying concentrations (1, 5, 10 and 20 μM). Assays were performed under similar conditions as employed for polymerization assays as described above [28].

3.2.3. Western blot analysis of soluble versus polymerized tubulin and cyclin B1

Cells were seeded in 12-well plates at 1×10^5 cells per well in complete growth medium. Following treatment of cells with respective compounds (**12b**, **12c** and **12d**) for duration of 24 h, cells were washed with PBS and subsequently soluble and insoluble tubulin fractions were collected. To collect the soluble tubulin fractions, cells were permeabilized with 200 μL of pre-warmed lysis buffer [80 mM Pipes-KOH (pH 6.8), 1 mM $MgCl_2$, 1 mM EGTA, 0.2% Triton X-100, 10% glycerol, 0.1% protease inhibitor cocktail (Sigma–Aldrich)] and incubated for 3 min at 30 °C. Lysis buffer was gently removed, and mixed with 100 μL of 3× Laemmli's sample buffer (180 mM Tris–Cl pH 6.8, 6% SDS, 15% glycerol, 7.5% β-mercaptoethanol and 0.01% bromophenol blue). Samples were immediately heated to 95 °C for 3 min. To collect the insoluble tubulin fraction, 300 μL of 1× Laemmli's sample buffer was added to the remaining cells in each well, and the samples were heated to 95 °C for 3 min. Equal volumes of samples were run on an SDS-10% polyacrylamide gel and were transferred to a nitrocellulose membrane employing semidry transfer at 50 mA for 1 h. Blots were probed with mouse anti-human α-tubulin diluted 1:2000 ml (Sigma) and stained with rabbit anti-mouse secondary antibody coupled with horseradish peroxidase, diluted 1:5000 ml (Sigma). Bands were visualized using an enhanced Chemiluminescence protocol (Pierce) and radiographic film (Kodak.). For cyclin B1 immunoblots, Cells were seeded in 12-well plates at 1×10^5 cells per well in complete medium and treated with different concentrations of **12b**, **12c** and **12d** for 24 h. After treatment, cells were washed twice with phosphate-buffered saline and lysed in 1X SDS sample buffer. Proteins were separated, transferred, probed and analyzed similar to tubulin. The primary anti-cyclin B1 antibody was employed at 1:1500 (Sigma) and horseradish peroxidase coupled goat anti-rabbit secondary antibody diluted 1:5000 (Sigma) [28].

3.2.4. Immunohistochemistry of tubulin and analysis of nuclear morphology

HeLa cells were seeded on glass cover slip, incubated for 24 h in the presence or absence of test compounds **12b**, **12c** and **12d** at a concentration of 5 μM. Cells grown on coverslips were fixed in 3.5% formaldehyde in phosphate-buffered saline (PBS) pH 7.4 for 10 min at room temperature. Cells were permeabilized for 6 min in PBS containing 0.5% Triton X-100 (Sigma) and 0.05% Tween-20 (Sigma). The permeabilized cells were blocked with 2% BSA (Sigma) in PBS for 1 h. Later, the cells were incubated with primary antibody for tubulin from (sigma) at (1:200) diluted in blocking solution for 4 h at room temperature. Subsequently the antibodies were removed and the cells were washed thrice with PBS. Cells were then incubated with FITC labeled anti-mouse secondary antibody (1:500) for 1 h at room temperature. Cells were washed thrice with PBS and mounted in medium containing DAPI. Images were captured using the Olympus confocal microscope and analyzed with Provision software.

3.3. Zebrafish maintenance and screening

Wild type zebrafish (Danio rerio) were raised and maintained at 28.5 °C with 14hr:10 h light : dark cycle. 2–3 pairs of zebrafish were synchronously mated and embryos were pooled. The embryos were dechorinated and 3–4 embryos were dispensed in 200ul of E3 embryo medium (5 mM NaCl, 0.17 mM KCl, 0.44 mM $CaCl_2$, 0.68 mM $MgCl_2$) into each well of a 96 well plate. The embryos were treated with the compound (10 & 25 μM), nocodazole (5 μM) or DMSO (1%) at 5 hpf and incubated at 28.5 °C. About 20 embryos were screened for each compound in biological replicates. They were observed after 28 hpf with a Leica stereomicroscope. Only those compounds that resulted in similar phenotypic defects in most of the embryos were considered as active [22].

3.4. Molecular modeling

AutoDock was used to dock 3,4,5-trimethoxybipheny derivatives in colchicine binding site of tubulin [24–26]. Initial Cartesian coordinates for the protein–ligand complex structure were derived from crystal structure of tubulin (PDB ID: 3E22). The protein targets were prepared for molecular docking simulation by removing water molecules, bound ligands. Hydrogen atoms and Kollman charges were added to each protein atom. Auto-Dock Tools (ADT) was used to prepare and analyze the docking simulations for the AutoDock program. Coordinates of each compound were generated using Chemdraw11 followed by MM2 energy minimization. Grid map in Autodock that defines the interaction of protein and ligands in binding pocket was defined. The grid map was used with 60 points equally in each *x*, *y*, and *z* direction. AutoGrid 4 was used to produce grid maps for AutoDock calculations where the search space size utilized grid points of 0.375 Å. The Lamarckian genetic algorithm was chosen to search for the best conformers. Each docking experiment was performed 100 times, yielding 100 docked conformations. Parameters used for the docking were as follows: population size of 150; random starting position and conformation; maximal mutation of 2 Å in translation and 50° in rotations; elitism of 1; mutation rate of 0.02 and crossover rate of 0.8; and local search rate of 0.06. Simulations were performed with a maximum of 1.5 million energy evaluations and a maximum of 50,000 generations. Final docked conformations were clustered using a tolerance of 1.0 Å root mean square deviation. The best model was picked based on the best stabilization energy. Final figures for molecular modeling were generated by using PyMol [27].

Acknowledgments

A.B.S, G.B.K thanks CSIR, New Delhi and C.K. thank the UGC, New Delhi for the award of senior research fellowships. We thank CSIR for financial support under the 12th Five Year plan project "Affordable Cancer Therapeutics" (CSC0301) and "Small Molecules

in Lead Exploration (SMiLE)" (CSC0111). We thank Dr. K. Ravinder for assistance with zebrafish assays.

Appendix A. Supplementary data

Supplementary data related to this article can be found at http://dx.doi.org/10.1016/j.ejmech.2013.10.077.

References

[1] M.A. Jordan, L. Wilson, Nat. Rev. Cancer 4 (2004) 253–265.
[2] C. Dumontet, M.A. Jordan, Nat. Rev. Drug Discov. 9 (2010) 790–803.
[3] E.A. Perez, Mol. Cancer Ther. 8 (2009) 2086–2095.
[4] M.A. Jordan, K. Kamath, Curr. Cancer Drug Targets 7 (2007) 730–742.
[5] F. Pellegrini, D.R. Budman, Cancer Invest. 23 (2005) 264–273.
[6] J. Caballero, C. Muñoz, J.H. Alzate-Morales, S. Cunha, L. Gano, R. Bergmann, J. Steinbach, T. Kniess, Eur. J. Med. Chem. 58 (2012) 272–280.
[7] R. Hoessel, S. Leclerc, J.A. Endicott, M.E. Nobel, A. Lawrie, P. Tunnah, M. Leost, E. Damiens, D. Marie, D. Marko, E. Niederberger, W. Tang, G. Eisenbrand, L. Meijer, Nat. Cell. Biol. 1 (1999) 60–67.
[8] M. Kritsanida, P. Magiatis, A.L. Skaltsounis, Y. Peng, P. Li, L.P. Wennogle, J. Nat. Prod. 72 (2009) 2199–2202.
[9] P. Singh, M. Kaur, W. Holzer, Eur. J. Med. Chem. 4 (2010) 4968–4982.
[10] Y. Zhong, M. Xue, X. Zhao, J. Yuan, X. Liu, J. Huang, Z. Zhao, H. Li, Y. Xu, Bioorg. Med. Chem. 21 (2013) 1724–1734.
[11] B. Abu Thaher, M. Arnsmann, F. Totzke, J.E. Ehlert, M.H. Kubbutat, C. Schächtele, M.O. Zimmermann, P. Koch, F.M. Boeckler, S.A. Laufer, J. Med. Chem. 55 (2012) 961–965.
[12] V. Krystof, P. Cankar, I. Frysová, J. Slouka, G. Kontopidis, P. Dzubák, M. Hajdúch, J. Srovnal, W.F. de Azevedo, M. Orság Jr., M. Paprskárová, J. Rolcík, A. Látr, P.M. Fischer, M. Strnad, J. Med. Chem. 49 (2006) 6500–6509.
[13] C. Wasylyk, H. Zheng, C. Castell, L. Debussche, M.C. Multon, B. Wasylyk, Cancer Res. 68 (2008) 1275–1283.
[14] C.M. Li, Z. Wang, Y. Lu, S. Ahn, R. Narayanan, J.D. Kearbey, D.N. Parke, W. Li, D.D. Miller, J.T. Dalton, Cancer Res. 71 (2011) 216–224.
[15] J. Chen, Z. Wang, C.M. Li, Y. Lu, P.K. Vaddady, B. Meibohm, J.T. Dalton, D.D. Miller, W. Li, J. Med. Chem. 28 (2010) 7414–7427.
[16] A. Kamal, G. Ramakrishna, P. Raju, A.V. Rao, A. Viswanath, V.L. Nayak, S. Ramakrishna, Eur. J. Med. Chem. 46 (2011) 2427–2435.
[17] S. Sidique, R. Ardecky, Y. Su, S. Narisawa, B. Brown, J.L. Millán, E. Sergienko, N.D. Cosford, Bioorg. Med. Chem. Lett. 19 (2009) 222–225.
[18] A. Kamal, J.R. Tamboli, M.V. Vishnuvardhan, S.F. Adil, V.L. Nayak, S. Ramakrishna, Bioorg. Med. Chem. Lett. 23 (2013) 273–280.
[19] M.A. Reddy, N. Jain, D. Yada, C. Kishore, J.R. Vangala, P. Surendra, R.A. Addlagatta, S.V. Kalivendi, B. Sreedhar, J. Med. Chem. 54 (2011) 6751–6760.
[20] L.I. Zon, R.T. Peterson, Nat. Rev. Drug Discov. 4 (2005) 35–44.
[21] H.S. Moon, E.M. Jacobson, S.M. Khersonsky, M.R. Luzung, D.P. Walsh, W. Xiong, J.W. Lee, P.B. Parikh, J.C. Lam, T.W. Kang, G.R. Rosania, A.F. Schier, Y.T. Chang, J. Am. Chem. Soc. 124 (2002) 11608–11609.
[22] C.B. Kimmel, W.W. Ballard, S.R. Kimmel, B. Ullmann, T.F. Schilling, Dev. Dyn. 203 (1995) 253–310.
[23] R.D. Murphey, H.M. Stern, C.T. Straub, L.I. Zon, Chem. Biol. Drug Des. 68 (2006) 213–219.
[24] AutoDock, version 4.0, http://www.scripps.edu/mb/olson/doc/autodock/.
[25] G.M. Morris, D.S. Goodsell, R.S. Halliday, R. Huey, W.E. Hart, R.K. Belew, A.J. Olson, J. Comput. Chem. 19 (1998) 1639–1662.
[26] R.B. Ravelli, B. Gigant, P.A. Curmi, I. Jourdain, S. Lachkar, A. Sobel, M. Knossow, Nature 428 (2004) 198–202.
[27] W.L. DeLano, DeLano Scientific, San Carlos, CA, USA, http://www.pymol.org, 2002.
[28] A.S. Kumar, M.A. Reddy, N. Jain, C. Kishor, T.R. Murthy, D. Ramesh, B. Supriya, A. Addlagatta, S.V. Kalivendi, B. Sreedhar, Eur. J. Med. Chem. 60 (2013) 305–324.